Dark Matter Searches at Colliders

Antonio Boveia[1] and Caterina Doglioni[2]

[1]Physics Department, The Ohio State University, Columbus, Ohio 43210, USA
[2]Fysikum, Division of Particle Physics, Lund University, 22363 Lund, Sweden

Annu. Rev. Nucl. Part. Sci. 2018. 68:1–34

https://doi.org/10.1146/annurev-nucl-101917-021008

Keywords

particle dark matter, invisible particles, weakly interacting massive particles, WIMPs, simplified models, colliders, LHC

Abstract

Colliders, among the most successful tools of particle physics, have revealed much about matter. This review describes how colliders contribute to the search for particle dark matter, focusing on the highest-energy collider currently in operation, the Large Hadron Collider (LHC) at CERN. In the absence of hints about the character of interactions between dark matter and standard matter, this review emphasizes what could be observed in the near future, presents the main experimental challenges, and discusses how collider searches fit into the broader field of dark matter searches. Finally, it highlights a few areas to watch for the future LHC program.

Contents

1. INTRODUCTION

Cosmological observations of dark matter (DM) are perhaps the most persuasive experimental evidence for physics beyond the Standard Model (BSM) of particle physics. DM may not be composed of particles at all, but the Standard Model of particle physics in describing ordinary matter gives us a strong reason to consider a particle description of DM as well.

Neverthless, the evidence for DM (described in, e.g., Reference 1), is inconsistent with the properties of any known particle. While DM has gravitational interactions with normal matter, DM particles are dark (see the sidebar titled Particle Properties of Dark Matter); its nongravitational interactions must be relatively rare. DM is very stable, with a lifetime comparable to that of the Universe (e.g. Reference 2). It is also nonrelativistic and collisionless. But most striking is its abundance at the present day [relic abundance (3)], extracted from measurements of the cosmic microwave background (4). There is approximately five times as much DM as the matter described by the Standard Model. This fact provides one of the few quantitative clues about BSM physics, and suggests that the complexity of the DM particle sector could match or exceed that of ordinary matter.

Particle physicists are increasingly keen to understand what DM is, if it is indeed composed of particles. Some experimenters, using direct detection (DD) experiments, look for Galactic DM colliding with underground targets made of ordinary matter (5). Others, using indirect detection (ID) experiments, search for the products of annihilating DM concentrated within the gravitational potential wells of the Milky Way and elsewhere (6). If the only interaction between DM and ordinary matter is gravitational, these experiments may never observe it directly. To succeed, both types of searches require that DM interact with ordinary matter in some way: DM–nucleon (or DM–electron) interactions in DD searches or DM annihilation to Standard Model particles in ID searches.

PARTICLE PROPERTIES OF DARK MATTER

1. Darkness: Most DM particle candidates produced in particle collisions are effectively invisible to traditional collider experiments. However, any remaining products of the collision event are not. Invisible particles can be accompanied by one or more visible recoiling particles, leading to missing momentum in the transverse plane, whose magnitude is termed $\not{E}_T$. This is one of the main signatures of DM in colliders.
2. Very long lifetime: If DM is a particle, it does not seem to decay. Conservation laws, such as those implied by Z_2 symmetry [e.g., R parity in supersymmetry (SUSY)], can prevent the DM particle from decaying into any lighter even-parity Standard Model particle. DM particles can also be produced in pairs by the decay of other particles, charged under the same gauge group as the Standard Model, or singly if the parent is a color triplet.

Colliders, among the most successful tools in particle physics, have revealed much about ordinary matter. If DM can be produced at colliders, they will likely remain one of our preferred tools for learning more about it, regardless of where DM particles are first discovered. As with DD and ID experiments, collider DM production relies upon the existence of interactions between the colliding Standard Model particles and the DM particles. If we can produce DM at the Large Hadron Collider (LHC) or its successors, we might begin to comprehend the forces that connect ordinary matter to DM, and to understand how the two interacted shortly after the Big Bang, leading to the Universe we see today.

This review describes how experiments at particle colliders contribute to the search for DM, focusing on the ATLAS, CMS, and LHCb experiments (7–9) at the highest-energy collider currently in operation, the LHC at CERN. The LHC results presented in this review include up to 36 fb^{-1} of proton–proton collision data recorded through 2017 during the 2015–2018 LHC run at 13-TeV center-of-mass energy (Run 2). This data set is almost twice as large as what was used for the Higgs discovery at 7- and 8-TeV center-of-mass energy (approximately 20 fb^{-1}) during 2010–2012 (Run 1), but it comprises only 1% of the 3,000 fb^{-1} expected with the full High-Luminosity LHC (HL-LHC) run, planned to start in 2026.

Given the absence of any hints as to the character of DM–Standard Model matter interactions, this review emphasizes what could be observed in the near future, presents the main experimental challenges, and discusses how collider searches fit into the broader field. Finally, it highlights a few areas to watch for the future LHC program.

2. REACTIONS FOR INVISIBLE-PARTICLE SEARCHES AT THE LHC

Just as neutrinos do, DM produced at colliders would almost always pass invisibly through the detector. In this section, we describe DM production from a pragmatic, collider physicist's perspective, focusing on a selection of simple models with distinct and testable LHC

signatures.[1] Moreover, we use the term invisible particles (rather than DM) when emphasizing that detecting such particles need not be a discovery of DM.[2]

The body of DM model literature can be divided into two extremes. Fully specified, self-consistent models such as SUSY provide specific features that can be exploited for narrowly targeted searches, while simplified models with a few components can capture broad collider signatures of classes of models, serving as benchmarks for more general but less optimal searches. Key to both are the determinative details of the interactions between DM and ordinary matter, rather than DM itself.

To restrict the scope of this review, we emphasize (*a*) models where the DM has an effective interaction with Standard Model particles such that it can be produced in colliders; (*b*) models that include Z_2 symmetry to stabilize DM; (*c*) models connecting to the most commonly studied cosmological history, where it is assumed that DM is in thermal equilibrium in the early Universe and freezes out to the current abundance [see Reference 10 for an overview; we briefly comment on others with alternate cosmological histories, which also have interesting signatures (11–13)]; (*d*) models in which the DM is a Dirac fermion; and (*e*) models that mimic the pattern of flavor violation found in the Standard Model, referred to as minimal flavor violation (MFV) (14). These are the models used in LHC Run 2 searches. Departures from these assumptions are discussed in Reference 15.

2.1. Higgs and Z Boson Portals

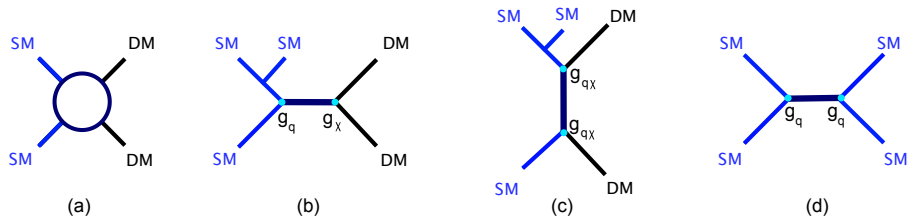

Figure 1

(*a*) The interaction between DM and Standard Model particles via an unspecified interaction (e.g., an EFT). (*b*) Examples of simplified model processes where the interaction is mediated by an intermediate particle (with additional radiation off one of the initial-state quarks). (*c*) The same model, in which the mediator decays back into Standard Model particles, with coupling constant g_q for the mediator–quark–quark vertex and constant g_χ for the mediator–DM vertex. Abbreviations: BSM, beyond the Standard Model; DM, dark matter; EFT, effective field theory; SM, Standard Model.

Extending the Standard Model with a single DM particle, one may arrive at models where the Higgs boson or the Z boson mediates the DM–Standard Model interaction, also called portal models. The Higgs boson and the Z boson in these models the are examples of mediators, particles governing the DM–Standard Model interaction. Figure 1*b*,*c* shows example Feynman diagrams.

[1] For other perspectives, see Literature Cited.

[2] For example, invisible particles may decay after leaving the detector, a decay that is essentially prompt on cosmological timescales.

Higgs portal models (16, 17) can be constructed by adding only DM and no other new particles to the Standard Model. Only the most recent recent generations of collider and DD experiments have reached the energies and luminosities necessary to search for such DM. Direct collider searches for the invisibly decaying Higgs bosons are augmented by measurements of other Higgs properties, which can be very sensitive to couplings to new particles.

Z portal models are strongly constrained by LEP and DD experiments (described in Reference 18 and Section 3.1). Either of these mediators (the Z or Higgs boson) is light in comparison to the LHC energy and can be produced on-shell, so collider searches may still constrain these models through precision studies of the visible decays of the Z and Higgs bosons, even if the invisible particles are much heavier and invisible decays of the mediator are absent.

2.2. Effective Field Theories and Simplified Models of Beyond-the-Standard-Model Mediators

More complex than the Z and Higgs portal models are models in which the mediator of the DM–Standard Model interaction is also a new particle, such as a heavier version of the Z boson (a Z') or an additional scalar.

2.2.1. Effective field theories. In some situations, such as when a BSM mediator is heavy compared with the collision energy, the DM–Standard Model interaction appears to be a contact interaction. All observables completely determined by one rate parameter, the contact interaction scale, that controls the production rate, and a Lorentz structure, which has a modest effect on the transverse momentum (p_{T}) distributions of the invisible particles. In this case, effective field theories (EFTs) (19–22) describe the production of invisible particles. Figure 1*a* depicts an EFT process. One may hope that such a description is sufficient for the LHC; the unknown high-energy details of a complicated interaction are conveniently integrated out. Moreover, since EFTs do not fix a mediation mechanism, they provide a framework to systematically explore a wide range of possible physics.

If, instead, the interaction physics is kinematically accessible (e.g., the mediator mass is within reach of the typical momentum transfer in the collision), one should replace the EFT description with a model specifying further details of the DM–Standard Model matter interactions (23). Without those details, however, one can still use the EFT language to obtain results for later reinterpretation once its high-energy completion is known (24, 25).

2.2.2. Simplified models. When the collision energy is near or higher than the mediator mass, complementary avenues to study the mediating interaction develop, analogous to the transition from the Fermi model of weak interactions at low energies to the Standard Model at higher energies. For example, at the LHC, a heavy neutral Z' mediator would often decay into the partons that produced it, and fully reconstructing such visible decays could provide more information about the interaction than the invisible decays alone. One can construct simple descriptions of collider phenomenology without including the details of additional physics at energies higher than the collider scales, and therefore not relevant at the LHC. These descriptions are termed simplified models (e.g., 26, 27), and can be considered an intermediate step the between simplest portal models and full theories.

Under the assumption that only a few new particles will be important in the early phase

The ATLAS/CMS Dark Matter Forum: provided the reference implementations of the models in Reference 15 (see `https://github.com/LHC-DMWG`) and implemented in models for various event generators [e.g., DMSimp (31)]

of discovery, simplified models can be developed for tree-level pair production of invisible particles. The set of such models currently employed for ATLAS and CMS searches is described in Reference 15, which builds upon much research from the wider DM community (e.g., 21, 28, 29). Although these simplified models often have to be embedded in a larger theory to satisfy theory constraints (30), in many cases they are sufficient to describe the leading-order collider phenomenology.

The standard models include models with neutral mediator particles singly produced at the LHC and decaying both to pairs of invisible particles and to pairs of Standard Model particles (Figure 1*b*,*c*). These two-body mediator decays offer simple, attractive benchmarks. Colored mediators allow vertices involving only one DM particle and phenomenology akin to that of SUSY models with a squark mediator (32–34). For additional decay signatures, for so-called dark sectors of many additional particles, and for LHC data sets far larger than at present, many more simplified models become interesting. Models of BSM mediation can be classified according to the spin of the mediator: spin-1 vector or axial–vector mediators (Z'), scalar mediators (referred to as ϕ below), and spin-2 mediators (35).

Massive color-neutral spin-1 bosons with vector or axial–vector couplings are nearly ubiquitous in BSM theories, so Z' bosons as the mediators connect with a wide class of models (23). Since the Z' coupling to quarks must be nonzero for its production at the LHC, both invisible and dijet signatures are discovery channels. This coupling (or loop-level coupling) to Standard Model partons is also required for nuclear recoils in underground DM searches.

The models in use at ATLAS and CMS contain vector, axial–vector, or mixed couplings to quarks and a single species of invisible particle. The couplings of the Z' boson (g_{q} to all quarks, g_ℓ to leptons, and g_χ to invisible particles), the mass of the invisible particle m_χ, and the Z' mass M_{med} are free parameters. Lepton decays, if not included explicitly at tree level, arise through the quark coupling at loop level (see Reference 36 and references therein). Decays of the spin-1 mediator into neutrinos are also required by gauge invariance, and add an invisible decay channel that can enhance signatures of missing transverse momentum, depending on the size of the couplings (36). The spin structure of the Z' couplings does not significantly change the LHC phenomenology, but it has a much greater effect in signals in noncollider searches. Figure 1*b*,*d* depicts an example process for this model for the case of invisible and visible decays, respectively. The rate of visible decays will increase quickly with increasing g_{q}. In order to show the interplay between the constraints from visible and invisible searches in different decay channels of the mediator, LHC searches adopt different benchmark coupling scenarios (described in Reference 36 and discussed in Section 3.5.1), where the coupling to DM is set to unity, the coupling to quarks is set to either 0.25 or 0.1, and the coupling to leptons is set to 0, 0.1, or 0.01. Those choices are made on the basis of the current LHC search sensitivity (see Section 3.5.1). These coupling values also ensure that the model is still perturbative in most of the parameter space tested by LHC searches (for a discussion of unitarity and gauge invariance for these models, see Reference 30) and that the mediator width is small compared with its mass.

Models mediated by a Z' boson can include additional couplings of the Z' boson to acquire mass through a new baryonic Higgs boson, h_B (37), through a coupling $g_{hZ'Z'}$. This model variant collapses to the simpler vector model above in the limit of very heavy Z' boson mass. Figure 2*a* shows an example Feynman diagram for this case. These models can also be embedded in a type II two–Higgs doublet model (2HDM) (37), as shown in Figure 2*b*.

With appropriate values of the model parameters, these models can satisfy the relic density constraints (38). However, taken in isolation, the axial–vector model is nonrenormalizable, and without additional ingredients perturbative unitarity is violated in certain regions of the parameter space (30, 38, 39).

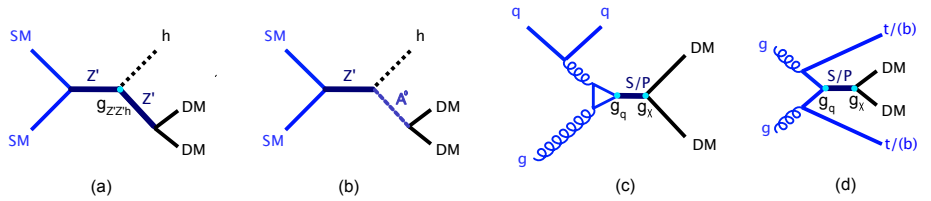

Figure 2

(a) Example of a process including baryonic coupling between a vector mediator Z' and an SM Higgs boson. The Z'–Higgs coupling is denoted $g_{hZ'Z'}$. (b) Example of a process from a $U(1)$ Z' boson embedded in a 2HDM, where a vector Z' decays to a pseudoscalar A^0 that in turn decays to DM particles. (c,d) Examples of a simplified model process where the interaction is mediated by an intermediate scalar or pseudoscalar particle. In panel c, the SM–scalar interaction proceeds through a gluon loop (86), whereas in panel d, the pseudo(scalar) is produced in association with a pair of heavy-flavor quarks. The coupling constants that are prefactors to the Yukawa couplings in the model are denoted g_{q} for the mediator–quark–quark vertex and g_χ for the mediator–DM vertex. Abbreviations: A^0/a, pseudoscalar bosons; b, bottom quark; DM, dark matter; g, gluon; h, SM Higgs boson; S, heavy scalar boson; SM, Standard Model; t, top quark; Z', vector mediator; 2HDM, two–Higgs doublet model.

Models including color-neutral scalar and pseudoscalar mediators (referred to as scalar mediators below) are analogous to the Higgs portal model, but with a BSM mediator. Figure 2c,d shows example Feynman diagrams for these cases. In comparison to the Z' models, a scalar mediator model (40) has some additional peculiarities. Under MFV, the couplings of the scalar bosons to fermions are mass dependent. As with the Higgs boson, there are three consequences: (a) mediator production through loop-induced couplings to gluons (41) and associated with heavy-flavor quarks (40), (b) production cross sections that are smaller than those for vector mediators, and (c) visible decays that are dominantly to third-generation quarks. Despite lower production cross sections, the lower backgrounds for these experimental signatures enable these models to be tested during LHC Run 2.

The collider phenomenology of the scalar models used by ATLAS and CMS is fully determined by the masses of the invisible particle and the mediator, the ϕ–invisible particle coupling (g_χ), and the ϕ–fermion (g_{q}) coupling. According to the convention used in Reference 15, g_{q} is a prefactor to the Yukawa couplings to fermions and is set equal for all quarks. For the same model parameters, the scalar and pseudoscalar models predict similar kinematic distributions at the LHC.

When introducing an additional scalar, one must consider how this new scalar relates to the Higgs boson. For example, large mixing with the Higgs can lead to strong constraints from Higgs measurements, when the scalar couples to DM through a Higgs portal (37). If the mediators are pure Standard Model singlets, then the model is not invariant under $SU(2)_L$ at the collider scale (42). Mixing with the Higgs sector is an example of how gauge invariance can be restored for these models. Couplings to the electroweak gauge bosons can also be added as a consequence of electroweak symmetry breaking (43, 44). The tree-level signatures in this case include Higgs or vector bosons plus missing transverse momentum

and, if the invisible particles are sufficiently light, invisible decays of the Higgs boson.

Colored scalar bosons allow direct coupling between Standard Model particles carrying color and invisible particles carrying Z_2 charge (32–34,45,46). Colored mediators can have a broader set of multijet signatures and kinematic features than the neutral mediator models, including the radiation of vector bosons by the mediator (34).

In colored scalar models, the mediator must be heavier than the invisible particle so as to ensure invisible-particle stability. For the current LHC results, the coupling between invisible particles and quarks ($g_{\chi q}$), the invisible-particle mass, and the mediator mass are free parameters.

The exchange of a scalar colored under $SU(3)$ is analogous to squarks in the minimal supersymmetric Standard Model (MSSM), in which only squarks and neutralinos are light. In the MSSM, the coupling between DM and the squark is constrained to be small (15). Without the requirements of a SUSY framework, this coupling need not be small. For example, if DM is a standard thermal relic, the couplings required to obtain the correct DM density are generally higher than those used by SUSY models.

2.2.3. Less-simplified models. Simplified models capture the typical features found in many models. As such, they can guide the design of generic searches, but may fail to describe the full complexity of possible collider signatures that arise in more complete models. By contrast, relying too heavily on a small sample of complete models risks focusing searches too narrowly on an unrepresentative set of signatures.

To solve this problem, many "less-simplified" models explore features that arise in special classes of models, finding a middle ground between too simplistic and unnecessarily complex. Because the set of such models grows quickly with the number of components, and because there is no broad consensus on which models should be a priority, very few of them have been explicitly considered by LHC searches. Here, we highlight a few such models with signatures different from those of the simplified models described above.

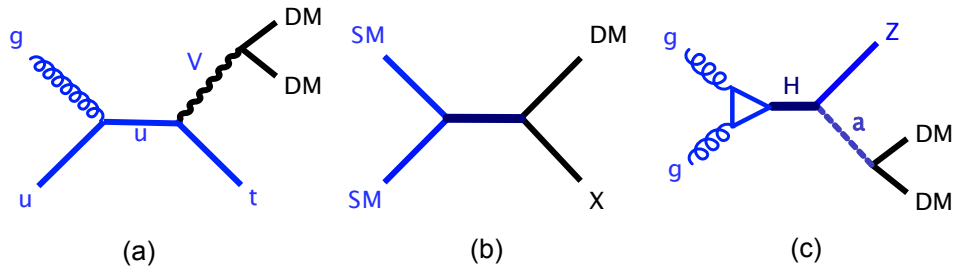

Figure 3

(a) Example of a process leading to a single top signature, proceeding through the coupling of a u and a t with a new vector boson, decaying to DM particles. (b) Example of a collider diagram from a coannihilation model, where two DM particles are present in the final state (one denoted DM and the other X). (c) Example of a diagram from a 2HDM process, with an interaction between an H, an SM Z boson, and an a mediating the SM–DM interaction. Abbreviations: a, pseudoscalar boson; DM, dark matter; g, gluon; H, heavy Higgs boson; SM, Standard Model; t, top quark; u, up quark; V, vector mediator; X, coannihilating DM partner, 2HDM, two–Higgs doublet model.

Models with more complex flavor violation structure than the Standard Model are just as motivated as those assuming MFV. But when constructing viable non-MFV models one must carefully evaluate many experimental constraints on flavor-violating processes (47). Mediators that couple to DM and a top quark appear in one category of flavor-violating model that remains least constrained by low-energy measurements (48). These yield a distinct "monotop" LHC signature, as shown in Figure 3*a*.

Coannihilation models add two species of dark sector particles with similar masses (see References 49 and 50 for examples). The interaction between these two states drives the cosmological history (3), as processes involving both types of particles can efficiently annihilate into Standard Model particles. LHC signatures include missing transverse momentum accompanied by multiple jets and/or by the decay products of the additional resonant particles in the model in addition to the invisible particle signatures, as in Figure 3*b*. The signatures can be very diverse, encompassing some typically considered in searches with very different motivation than DM (e.g., searches for leptoquarks). In some cases, these signatures have not received much attention from any current LHC search (49).

Ultimately, we do not yet know whether the Standard Model Higgs boson is alone in the scalar sector, nor whether a single scalar mediator encodes all of the important features of the complicated phenomenology of more complex scalar sectors. A step beyond the simple scalar mediator model, dictated by gauge invariance, is to take mixing between this mediator and the Standard Model Higgs boson into account (37, 43). A much larger step beyond that is to consider an extended Higgs sector such as a 2HDM, in which one or more of the scalars acts as the mediator between DM and ordinary matter (42, 51, 52). In such models, the new mediator mixes with the Higgs partners rather than with the Standard Model Higgs boson, so the model remains compatible with Higgs measurements. Some models developed for LHC searches focus on one Yukawa structure (type II) (53). Their particle content includes two *CP*-even bosons (of which one is the Standard Model Higgs boson), two *CP*-odd bosons (of which one is the pseudoscalar DM mediator), two charged Higgs bosons, and the invisible particle. Masses and couplings of these models are chosen to respect vacuum stability (52) as well as electroweak and flavor constraints, and to reproduce the observed DM abundance. Figure 3*c* shows an example Feynman diagram.

One can keep going further in this direction. For example, models with multiple mediators having small couplings to Standard Model particles have been developed to evade existing LHC constraints from DM searches (54).

2.3. Supersymmetric Models and Other Complete Theories

So far, we have considered rather general simplified models inspired by the electroweak sector of the Standard Model. Obviously, there are many more possibilities. Additional sources of inspiration for searches are the large number of BSM theories that have been developed to solve theoretical problems of the Standard Model as well as the mechanisms through which these provide invisible particles.

SUSY is one such class of theories, postulating partner particles to all Standard Model degrees of freedom. Supersymmetric models can stabilize the mass of the light Higgs boson and introduce desired features in the Standard Model, such as coupling unification. Reviews of supersymmetric DM models can be found elsewhere (55). Here, we broadly sketch models relevant to recent experimental progress and emphasize areas where we expect future developments.

Supersymmetric DM, the archetype for the concept of weakly interacting massive particles (WIMPs), has a long history (56). The most viable and well-studied type of supersymmetric DM has been neutralino DM. The neutralino, a partner particle to the Standard Model gauge bosons, is often assumed to be the lightest supersymmetric particle (LSP). R parity conservation makes the LSP stable (57) and prevents proton decay.

In the MSSM, there are four neutralinos, each of which is a mixture of Standard Model boson superpartners: a wino, a bino, and two higgsino fermion states. The lightest neutralino may be called bino-like, wino-like, or higgsino-like in regions of MSSM parameter space where one of these components dominates the mixture. The phenomenology of the neutralinos is different from that of most of the simplified models described in the previous section, and it depends on the mixture and on the particle spectrum. The LHC signatures feature missing transverse momentum from the neutralino and a high multiplicity of other objects (leptons, jets) produced in cascade decays of heavier superpartners.

The MSSM is a complete theory with more than 100 independent parameters, but viable SUSY models might be far simpler. Such models are used as predictive benchmarks for DM searches. One such model is the phenomenological MSSM (pMSSM), which assumes no sources of *CP* violation beyond the Standard Model and no flavor-changing neutral currents, and retains universal couplings and masses for first- and second-generation superpartners, reducing the number of MSSM parameters to 19.

Another DM candidate, found in gauge- or gravity-mediated supersymmetric models, is the gravitino, a spin-3/2 particle superpartner of the graviton. Gravitino interactions are suppressed by the Planck scale (10^{18} GeV) before SUSY breaking. This has consequences both for the viability as a thermal relic and for the phenomenology of these models. In gauge-mediated SUSY, the gravitino can be a DM candidate for a nonstandard cosmological history (58). Similar to the neutralino case, the identity and masses of heavier states decaying to the gravitino LSP determine the gravitino's phenomenology. However, the gravitino's interactions are very weak, posing problems for both DD and ID searches.

Because of the wide variety of potential experimental signatures, SUSY searches often adopt a simplified model approach, decoupling the particles that determine the lowest-energy collider phenomenology [generally the LSP and the next-to-lightest supersymmetric particle (NLSP)] from the rest of a heavier particle spectrum (27). As in the general simplified models described above, extending the MSSM quickly generates a plethora of nonminimal possibilities.

2.4. Long-Lived Particle Models

Another class of models, found within and beyond SUSY, feature suppressed cascade decays of a heavier particle (the NLSP in SUSY) to a lighter particle (the DM LSP in SUSY). The suppression can be so large that the particle travels a macroscopic length within the detector before it decays. Such particles are known as long-lived particles (LLPs).

LHC detectors are not optimized for this purpose, and additional work is required for searches to be sensitive. For example, within SUSY one way to suppress decays is for the NLSP to decay through a heavy intermediary. Split SUSY models are a subset of SUSY models in which the gluino must decay through a heavy, off-shell squark (59). The heavier the mass of the squark is, the longer lived the gluino will be. Alternatively, the NLSP decay can be heavily suppressed by some power of the mass difference with the LSP. This mass difference also affects DM coannihilation rates and therefore the DM

abundance (3). Another way to achieve long-lived decays is with parametrically small couplings, as in the case of gauge-mediated SUSY models wherein the long-lived NLSP decays to its Standard Model partner plus the gravitino (58), in a SUSY analog of Cabibbo-suppressed B meson decays in the Standard Model. Because of the prevalence of these mechanisms, it is important to look for long-lived cascade decays.

In addition to SUSY, small couplings can also lead to find long-lived signatures within the generic simplified models described in Section 2.2.2. The early Universe mechanism that is responsible for the observed DM density is not known. If one assumes thermal freeze-out, then the coupling of the mediator to DM pairs cannot be arbitrarily small. In alternate scenarios, such as so-called dark freeze-out in which DM can annihilate directly to BSM mediators but not vice versa, the mediator couplings to the Standard Model can be much smaller (13,60,61). The freeze-in scenario (11,62) is another possibility for reproducing the observed relic density in presence of very weak DM–Standard Model matter interactions, but LHC rates for some of these models may be too small for observation (63).

Despite the small couplings, a sufficiently light mediator can be produced at colliders with an appreciable cross section. Many such models have been proposed, and here we sketch only a few. For example, DM can interact with the Standard Model via a dark vector boson of a $U(1)'$ dark symmetry, equivalent to the Standard Model's $U(1)$ but with much smaller couplings (64), such as those that originate from kinetic mixing. The mediator can also be a dark scalar boson (a so-called dark Higgs) that couples only to the Standard Model, akin to a Higgs portal (65). In both cases, the dark boson mediator can be light and long lived (60), and its visible decays into Standard Model particles or associated production with a Standard Model boson provides the main collider handle for observation (65). These scenarios can also be probed by complementary beam-dump and fixed-target experiments (66). Simplified coannihilation models with long-lived particles have also been proposed (67).

2.5. Dark Interactions

In the above subsections, we have sketched some of the models and signatures that are currently being sought at colliders. However, we have not covered many models. To an extent, any model containing stable particles interacting feebly with the Standard Model is a theory of DM. The key differences between models of DM and other models of BSM physics are the connections between these models and astrophysical DM.

The dark sector can be arbitrarily complex, as long as the particles and interactions it contains satisfy cosmological observations (13, 68). The models listed above are simple examples of such dark sectors, where the mediator particles (e.g., dark bosons) provide the connection with the Standard Model. Many other models are worthy of mention here, including asymmetric DM models, in which dark sector particles and antiparticles are not produced in equal amounts, in the same fashion as matter and antimatter for Standard Model baryons (69); models of neutral naturalness that realize a mirror copy of the Standard Model without any low-mass equivalent of the SUSY colored partners (70); and models of strongly interacting massive particles (SIMPs) with to sub-GeV DM candidates (71).

3. EXPERIMENTAL RESULTS

The interactions described in the previous section have many consequences for astrophysics (where they could modify the DM density) and for collider and noncollider particle physics experiments. Collisions of known particles at high energy, observed with well-understood detectors, have led to the discovery of many of the fundamental components of known matter in the Standard Model. While collider experiments alone cannot discover DM, they can discover the existence of invisible particles, which could lead the way to direct study of DM–Standard Model matter mediators in other channels and of additional particles in a dark sector.

DM–Standard Model matter interactions may be feeble because they are mediated by a heavy mediator or by a mediator with small couplings to Standard Model. Many high-energy collisions are needed to extensively search for these interactions, and the LHC, which presently collides protons at a center-of-mass energy of 13 TeV, will deliver both in the coming years.

Below, we outline how the relevant searches are done, some of the challenges, and the information the searches provide about the properties of hypothetical particles (couplings, mediator mass, other parameters of the Lagrangian in a particular model). In Section 4, we describe how collider information can be related to noncollider DM searches and to the present DM abundance.

3.1. Searches for Invisible-Particle Production Mediated by Standard Model Bosons

Colliders have already provided spectacular evidence for copious production of low-mass invisible particles: the huge rate of neutrino production mediated by the W and Z bosons. As a result, neutrino production via the Z boson is often the largest background to searches for new invisible particles and is important to understand well. The rate of events with considerable p_{T} is predicted by the Standard Model. The data would show a significant deviation from this prediction if the Z boson were coupled to additional invisible particles lighter than approximately half its mass. The most precise measurement of the invisible Z boson's width, 499.1 $\pm$ 1.5 MeV, has been inferred from the total Z width at LEP (72). This value can be used to constrain the parameters of models such as Z portals (18, 73), where the coupling between the Z boson and an invisible Dirac fermion, lighter than the Z mass, is constrained to be significantly smaller than the values necessary for a thermal relic. A less precise direct measurement of the Z boson's invisible width, also by LEP, uses invisible decays with a photon emitted as initial-state radiation (ISR), selecting events with a single photon, the total missing transverse momentum inferred from momentum balance with the visible particles ($\not{E}_T$), and little other event activity. At the LHC, precision measurements continue to test the production and decay of Z bosons for the effects of invisible particles. For example, ATLAS has measured the ratio of cross sections for jet and $\not{E}_T$ production, dominated by invisibly decaying Z bosons, to the production of Z bosons decaying to dilepton pairs, a ratio that is sensitive to the production of additional invisible particles (74).

Invisible decays of the newly discovered Higgs boson are, in the Standard Model, decays to a pair of Z bosons that then each decay invisibly, contributing to less than 0.1% of the total width of the Higgs boson. With present data, the Higgs-to-invisible rate could become observable if the Higgs is coupled to additional invisible particles (75, 76). To constrain the

MEASURING INVISIBLE PARTICLES: $\not{E}_T$ RECONSTRUCTION

Measurements of $\not{E}_T$ in experiments at hadron colliders should include contributions from all particles in the event, and therefore rely on precise measurements in all detector systems. The calculation of $\not{E}_T$ includes all visible physics objects (e.g., jets, leptons reconstructed from energy deposits and tracks) from the hard scatter interaction. Contributions that are not attributed to physics objects form the soft component of the $\not{E}_T$ (81, 82).

A challenge for $\not{E}_T$ measurements is to exclude contributions from the debris of additional proton–proton interactions detected at nearly the same time as the hard scatter (pileup). The combination of tracking and calorimeter information is used to identify tracks and energy deposits that originate from the primary collision vertex (82, 83).

A further challenge for the measurement of invisible particles is the rejection of fake missing transverse momentum. Noncollision backgrounds, such as cosmic rays, beam background, and detector noise, make a significant contribution to the tails of the $\not{E}_T$ spectrum (Figure 4). Specific quality cuts, based on the presence of tracks associated with the deposited energy and on the energy deposited in the various calorimeter layers, are applied to reject these events (84). For example, the number of events passing the jet+$\not{E}_T$ analysis selection before these quality cuts is approximately 10 times larger than the Standard Model contribution in Reference 85.

invisible width of the Higgs, ATLAS and CMS cannot directly measure its total width in a model-independent fashion (77); instead, searches attempt to directly observe these decays via their recoil against visible particles (resulting in substantial $\not{E}_T$) or through a comparison of measurements of the Higgs parameters under additional assumptions about the BSM physics. Direct Higgs-to-invisible searches have used Run 1 and Run 2 data, combining several strong and electroweak production channels. A combination of DD and ID searches yields the most stringent upper bound on the fraction of invisible decays of the Higgs boson: 23% (76, 78). For Dirac invisible particles much lighter than half the Higgs mass, this places constraints on Higgs portal couplings that are smaller than those necessary for a thermal relic, indicating that, even if this model with these parameters is realized in nature, additional sources of DM are needed.

3.2. Generic Searches for Invisible Particles from Beyond-the-Standard-Model Mediation

Searches for invisible decays via a Standard Model mediator (the Z or Higgs boson) can be viewed as special cases of searches for more general BSM mediation of invisible particles. Mediator decays to invisible particles are suppressed if the invisible-particle mass is heavier than half the mediator mass. For the case of the Z or H boson–mediated interactions, the upper bound for invisible particle masses that can be observed is ∼45–65 GeV. Moreover, the distribution of $\not{E}_T$ in events with a mediator with masses comparable to the H and Z has a similar shape to that of the Z boson–mediated neutrino background.

For heavier BSM mediators, this is not necessarily the case. Their decay to invisible particles can produce $\not{E}_T$ distributions substantially different from the Standard Model background. The complexity of the processes mediating invisible-particle production deter-

mines the composition of the visible recoil, so searches are employed across many different visible-particle signatures. Because of the large number of model possibilities, many collider searches, from LEP to the Tevatron to the most recent LHC searches (e.g., 20,79), aim to be model agnostic, designed to detect an excess of $\not{E}_T$ over the Standard Model background with minimal assumptions about the visible objects in the recoil. For this reason, the ISR+$\not{E}_T$ has become a key signature for invisible-particle searches at colliders and has gained popularity since its use at LEP (80).

We begin with the jet+$\not{E}_T$ search, which illustrates techniques used in other general invisible-particle searches and shares with them many of the same challenges in measuring $\not{E}_T$ (some of which are outlined in the sidebar titled Measuring Invisible Particles: $\not{E}_T$ Reconstruction). Traditionally, these have been called mono-X searches, but the radiation of a single object is only the leading process in the simplest reactions (86).

Only a fraction of proton–proton collision events can be recorded for further processing. The selection of those events (termed triggering; see Reference 87 for a review of the ATLAS and CMS systems and Reference 88 for LHCb) needs to happen in real time. This selection can be done in a model-agnostic way by looking for substantial $\not{E}_T$; however, for models that do not produce large $\not{E}_T$, one is forced to assume more about the visible recoil, as described in the rest of this section.

3.2.1. Searches with jets. One way to reduce the model dependence of DM searches at colliders is to require that the recoiling visible particles be governed by Standard Model processes, not by the dark interaction, so their relative rates and spectra are predictable with no model assumptions. ISR meets this criteria. Standard Model bosons are likely to be present in any BSM process, radiated from initial-state partons at rates fixed by the Standard Model. Because gluon ISR is far more prevalent at hadron colliders than the other forms, the jet+$\not{E}_T$ search is key in this approach.

LHC jet+$\not{E}_T$ searches (89,90) typically selects collision events with a moderate amount of $\not{E}_T$ (above roughly 200 GeV in the 13 TeV analyses in order to trigger at a manageable rate; see the sidebar titled Challenges for Triggering Low-Mass Resonances at Hadron Colliders) and at least one jet with p_{T} higher than 100–200 GeV in the central region of the detector (with pseudorapidity $|\eta| < 2.4$). From this sample, further restrictions on additional hadronic jets and other visible particles are used to suppress contributions from Standard Model processes and from instrumental backgrounds causing spurious $\not{E}_T$. These requirements reduce the generality of the analysis but also better isolate signal-like events. For example, contributions from W bosons decaying to leptons are reduced by vetoing events with leptons, and top quark pair production is reduced by limiting the number of jets present. The remaining Standard Model multijet processes can exhibit high $\not{E}_T$ when one or more jets are mismeasured. Such mismeasurements often result in $\not{E}_T$ along the axis of a jet, and this feature is used to reduce the background to approximately 1% of the total. Noncollision events (e.g., intersecting cosmic rays, beam–gas interactions, and calorimeter problems) can also produce spurious $\not{E}_T$. Figure 4 shows that such events dominate a high-$\not{E}_T$ data sample unless they are rejected with criteria tailored to the expected collision time and detector hardware.

After the above criteria are satisfied, one arrives at a sample composed mainly of invisible decays of the Z boson (approximately 55–70% of the total background). A substantial rate of semileptonic decays of the W boson also survives the lepton veto when the lepton is not reconstructed (approximately 20–35% of the total background. The main observable is

CHALLENGES FOR TRIGGERING LOW-MASS RESONANCES AT HADRON COLLIDERS

The LHC collides protons every 25 ns in nominal conditions. The decision to record collision events for further analysis is made by each experiment's trigger system (87, 88, 91, 92). Its first, hardware-based level uses partial detector information for fast decisions. Its second, software-based level uses more refined algorithms and has access to further detector information.

A challenge for many DM searches at colliders is to trigger on events with low-p_{T} objects. The trigger system records events above a certain threshold (e.g., leading-jet p_{T} or event $\not{E}_T$), since energetic processes are likely to contain interesting features. Only a small fraction of events below these thresholds is recorded, penalizing signals with lower-energy signatures. However, if only final-state objects reconstructed by the trigger system are recorded, instead of full event information, the storage limitations can be overcome (93–95). Alternative strategies to access resonances with masses below the TeV are to trigger on the ISR or selecting lower-backgrounds heavy quarks in the final state, as described in the text.

Pileup can add energy uncorrelated to the hard process of interest, increasing the event rate for a given trigger threshold; trigger $\not{E}_T$ rates increase exponentially with the number of additional interactions. For this reason, increases in LHC instantaneous luminosity and data set size come at the cost of increased thresholds. Dedicated pileup suppression algorithms, including partial tracking information, are used in trigger reconstruction (83,96). ATLAS and CMS foresee dedicated hardware systems to obtain full tracking information in future LHC runs (97,98).

typically the number of events in one or more $\not{E}_T$ regions with events selected to be enriched in contributions from signal processes (signal regions). Signal regions are either exclusive (in bins of $\not{E}_T$) or inclusive (considering all events above a given $\not{E}_T$ threshold).

Because invisible particles have feeble interactions with the colliding partons, and thus low production cross sections, these searches need precise estimates of the shapes of the backgrounds, especially in the low-$\not{E}_T$ regions. A background estimate made solely on the basis of Monte Carlo simulation is subject to uncertainties in both theory and detector simulation affecting the total cross sections, and therefore is not precise enough. Recent ATLAS and CMS searches combine the information from data in signal-free control regions selecting visible-boson (W, Z, γ)+jet processes with the most recent perturbative calculations (99), to estimate the Z- and W-mediated neutrino backgrounds more precisely. ATLAS estimates backgrounds from top processes using a control region with b jets, while CMS takes this background from simulation. Estimates of smaller backgrounds rely more heavily on simulation.

Currently, the precision achieved for the background estimate is 2–7% (CMS) and 2–10% (ATLAS), depending on the $\not{E}_T$ range. The remaining uncertainties arise mainly from the identification of leptons (CMS) and the understanding of jet and $\not{E}_T$ calibration (ATLAS). With no excesses observed, these searches set 95%-CL limits on the production cross section of invisible particles, typically ranging from 0.5 pb to 2 fb, depending on the $\not{E}_T$ threshold.

ATLAS and CMS report constraints for a selection of mediator models and parameters. These constraints are strong enough to probe (axial–)vector mediated processes, but searches are only becoming sensitive to lower cross-section scalar mediated processes. These constraints can be interpreted as limits on the interactions between the mediator and the Standard Model (e.g., g_{q}) under specific sets of model assumptions, not on the mass and

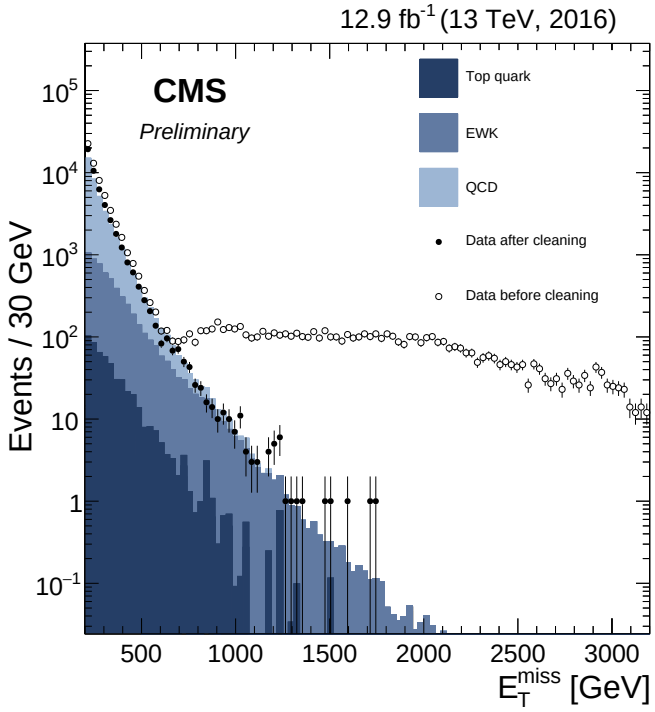

Figure 4

The $\not{E}_T$ distribution of events, selected for high total hadronic energy and at least two jets with $p_T > 400$ and 200 GeV, before (*open circles*) and after (*filled circles*) rejection of spurious $\not{E}_T$ backgrounds (82). The predictions of Monte Carlo simulations (*shaded areas*) are also shown. Strong noncollision background suppression is vital to $X+\not{E}_T$ analyses.

other properties of the invisible particles per se. As an example, for the simplified model with (axial–)vector mediators, mediator masses of up to 1.5–1.9 TeV are ruled out for an invisible coupling of $g_\chi = 1$ and $g_q = 0.25$. For mediators lighter than this bound, the search can exclude Standard Model couplings of order 0.1 or, alternatively, lower g_χ values than unity. With this amount of data, the searches are also becoming sensitive to lower-rate interactions mediated by scalar mediators, and the ATLAS search (89) sets explicit constraints on colored scalar mediators, where, for unit couplings and invisible particle masses of up to 100 GeV, the mass of the mediator is constrained to be above 1.7 TeV. Jet+$\not{E}_T$ results from LHC Run 1 and the Tevatron have also reported constraints on EFT models.

Since this type of search can constrain a wider variety of interactions than explicitly considered, steps have been taken to allow easy reinterpretation of the results. ATLAS and CMS provide more detailed experimental results on the HEPData platform (100). CMS also provides a simplified likelihood function encapsulating the result (90, 101).

3.2.2. Searches with photons and vector bosons. Particles other than gluons can constitute visible-particle recoil. In models where the recoil arises from ISR, the rates for photon and electroweak boson radiation are much smaller than for gluon radiation. Neverthe-

less, searches in photon+$\not{E}_T$ and Z+$\not{E}_T$ channels can play a complementary role alongside jet+$\not{E}_T$ searches, with a smaller and different mix of backgrounds and different systematic uncertainties. Both ATLAS and CMS have performed searches in each channel. With lower backgrounds, events can be recorded with lower kinematic thresholds, resulting in lower $\not{E}_T$ and visible-p_{T} selections. For example, the lowest $\not{E}_T$ value probed by the Z+$\not{E}_T$ search, where the Z decays into leptons (102, 103), is around 100 GeV, versus 200 GeV for the jet+$\not{E}_T$ search (90).

These searches can play a much more powerful role when the recoil arises from the dark interaction itself rather than ISR. In these cases, photon or vector boson recoil (e.g., 80, 104,105), rather than gluon recoil, may be the dominant signature. The event selection and the background estimation strategies generally mirror those of the jet+$\not{E}_T$ search, but vary with the type of recoil, taking advantage of the special features of the signal. Photon+$\not{E}_T$ searches (106,107) has lower backgrounds with respect to the jet+$\not{E}_T$ searches and therefore retains a comparable albeit lower sensitivity.

Some searches look for more complex recoil features. For example, the searches for signatures of hadronic decays of high-p_{T} electroweak bosons recoiling against sizable $\not{E}_T$ take advantage of the boson boost to reconstruct its collimated decay products in a single, large-radius jet (90, 108). Vector boson jets have a typical two-prong pattern from the hadronization of the quark–antiquark pair, while QCD jets do not present any structure. Substructure techniques (see Reference 109 for a review) are used to discriminate between these two cases.

None of the photon and vector boson+$\not{E}_T$ searches have yet observed a signal. These searches are generally not as sensitive as the jet+$\not{E}_T$ search to models in which the visible recoil arises from ISR, because of smaller signal acceptance and a comparable signal-to-background ratio. Nevertheless, they can be remarkably competitive: The photon+$\not{E}_T$ searches are the next-most-powerful probe after the jet+$\not{E}_T$ searches. Moreover, these searches provide the most stringent limits on some models in which the boson in question is directly involved in the dark interaction (37).

3.2.3. Search signatures including the Higgs boson. One can also look for the newly discovered Higgs boson in the recoil. Due to the heavy mass of the Higgs and the small heavy-flavor content of the proton, the rate of Higgs ISR is insignificant. Thus, searches for Higgs+$\not{E}_T$ target dark interactions in which the Higgs is a direct participant and, therefore, the interaction is closely tied to the Higgs sector. This is a feature of many models that extend the Standard Model scalar sector, such as those described in Sections 2.2.2 and 2.2.3.

Dedicated searches for Higgs+$\not{E}_T$ select Higgs events similarly to the inclusive Higgs measurements, then require substantial $\not{E}_T$ to reduce the backgrounds to the search. In the Run 2 data, searches in the $H \to \gamma\gamma$ (110, 111) and $H \to b\bar{b}$ (112) channels have been performed. Searches in the ZZ, WW, and $\tau\tau$ channels are expected to contribute as well, once substantially more data have been collected.

The $\not{E}_T$ +$H \to \gamma\gamma$ searches (110,111) benefit from their ability to precisely constrain the diphoton pair to the Higgs boson mass. They are still statistically limited. The relatively low backgrounds enable probing for anomalous $\not{E}_T$ as low as 50 GeV (110). The diphoton-invariant mass is fitted in different signal categories, each optimized for different types of signal models. The search for a Higgs boson decaying to two bottom quarks (112) requires $\not{E}_T$ >150 GeV. All backgrounds except for the QCD background are estimated using Monte Carlo simulation and constrained in dedicated control regions. This search also employs jet

substructure techniques for $\not{E}_T$ >500 GeV to select boosted Higgs decays amid a background of QCD processes. The main systematic uncertainty for the lower-$\not{E}_T$ signal region is the modeling of the V+jets background, while a higher-$\not{E}_T$ signal region is still statistically limited with the current data set.

In the absence of a signal, limits are placed on the baryonic Higgs benchmark model (outlined in Section 2.2.2 and shown in Figure 2*c*) with $g_q = 1$, $g_\chi = 1$, and $g_{hZ'Z'}/m_Z = 1$, and on a Z'–2HDM (Figure 2*d*). [3] Higgs+$\not{E}_T$ and Z+$\not{E}_T$ searches are also sensitive to extended scalar sectors such as two Higgs doublets with a scalar or pseudoscalar mediator (42, 51, 52).

3.2.4. Searches with third-generation quarks. In scalar- and pseudoscalar-mediated simplified models, the mediator can be produced along with two top or bottom quarks, leading to a signature that includes $\not{E}_T$ and multiple b jets. A recent ATLAS search in these channels (113) is optimized for both recoil consisting of semileptonic and fully hadronic top quark decays and recoil with one or two bottom quarks. This signature is similar to that of third-generation quark superpartners and can be part of dedicated SUSY searches or used for reinterpretation (114, 115). SUSY searches suppress most of the $t\bar{t}$ background, matching specific models to specific, low-background signal regions. Relative to these approaches, the search described in Reference 113 is less narrowly targeted at specific models, where control regions can be more reliably developed, instead relying more heavily on simulation. The sensitivity of searches of $\not{E}_T$ associated with top quarks is comparable for the two strategies.

No significant excess is observed in these searches. For invisible-particle masses of 1 GeV, color-neutral pseudoscalar mediators with masses in the range of 20–50 GeV (114) and scalar mediators with masses up to 100 GeV (115) are excluded. Signatures with $b\bar{b}$ pairs are less sensitive to models that do not explicitly privilege bottom quarks, but they can set much higher limits on colored mediator masses in the case of preferential couplings to bottom quarks (116).

Other LHC searches in this category are those including only one top or bottom quark (also called monotop or monobottom searches) (117, 118). They place constraints on models that include singly produced invisible particles through flavor-changing neutral currents (48).

3.3. Searches for Supersymmetric Invisible Particles

So far motivated by simple models, the X+$\not{E}_T$ experimental searches discussed make few choices about the visible recoil particles (i.e., the species of a single particle), yet they have already led to a plethora of diverse signatures. Models with more degrees of freedom vastly expand the set of signatures to be explored. SUSY adds, along with invisible particles, a full copy of the Standard Model particle spectrum to be discovered. Each superpartner features particular decay chains that can be targeted to a greater or lesser degree, privileging either generality or maximal sensitivity. Compared with the searches described above, SUSY searches generally opt for a more specific decay topology and thus apply more stringent event selections based on the expected kinematic features, often using discriminating variables

[3] In the case of the Z'–2HDM, CMS and ATLAS set different masses for the new Higgs bosons, so the constraints are not yet directly comparable.

based on the combined mass of visible and invisible particles (e.g., 119) to recover the ability to resolve various resonant decays.

SUSY has received much attention from ATLAS and CMS, and many searches for its particles, such as for squarks and gluinos, have a long history at earlier colliders as well. In this section, we discuss experimental results with explicit connections to DM.

So far, no SUSY search has produced a conclusive signal. However, given its multifarious signatures, it is difficult to make general statements about the current status, even for simplified models of SUSY. Perhaps the best one can say is that searches for strongly produced superpartners constrain them for masses approaching ∼2 TeV for neutralino masses up to 1 TeV (e.g., 120, 121); by contrast, other processes are less constrained. Direct production of weakly coupled superpartners has a much smaller production rate; therefore, the constraints on them are significantly weaker, as shown in Figure 6. Third-generation squarks are generally only constrained to be at least several hundred GeV for neutralinos of similar masses (e.g., 122, 123). But there are numerous exceptions to these blanket statements, even before one takes into account that the masses exclusions shown in Figure **??** apply only to specific slices of a multidimensional model parameter space.

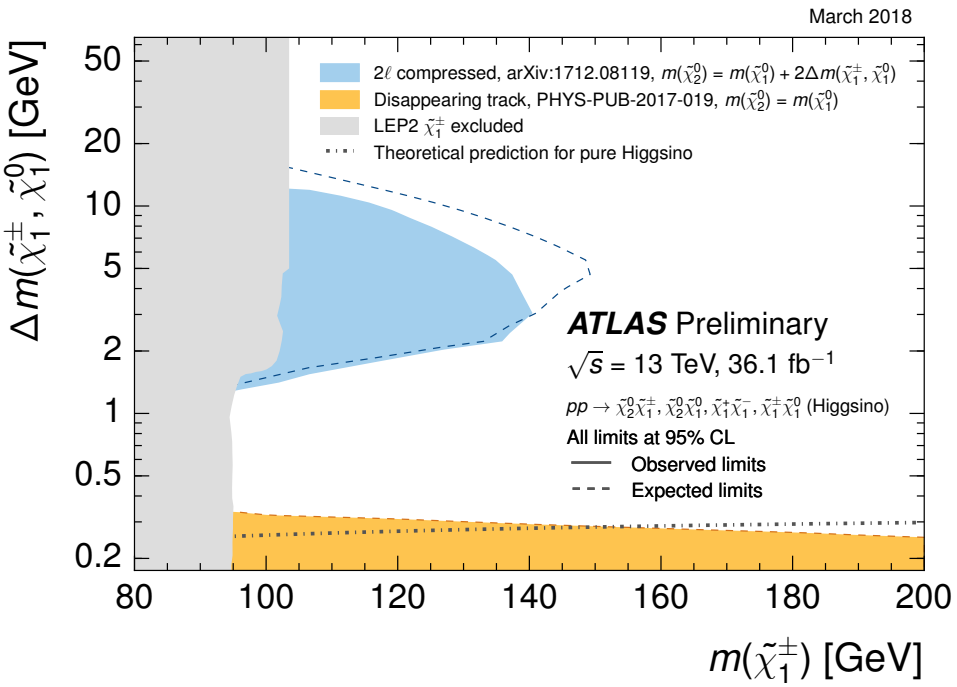

Figure 5

Mass reach of ATLAS searches for a selection of results targeting electroweak supersymmetry production, available as of December 2017 (125).

Although LHC searches have so far probed mainly SUSY channels that are strongly produced, searches for more rare processes are now entering their prime. With the data now collected, one can explore the electroweakino parameter space (e.g., 126, 127). Searches for gauge boson superpartners (gauginos) can reach approximately 1 TeV if the superpartners of

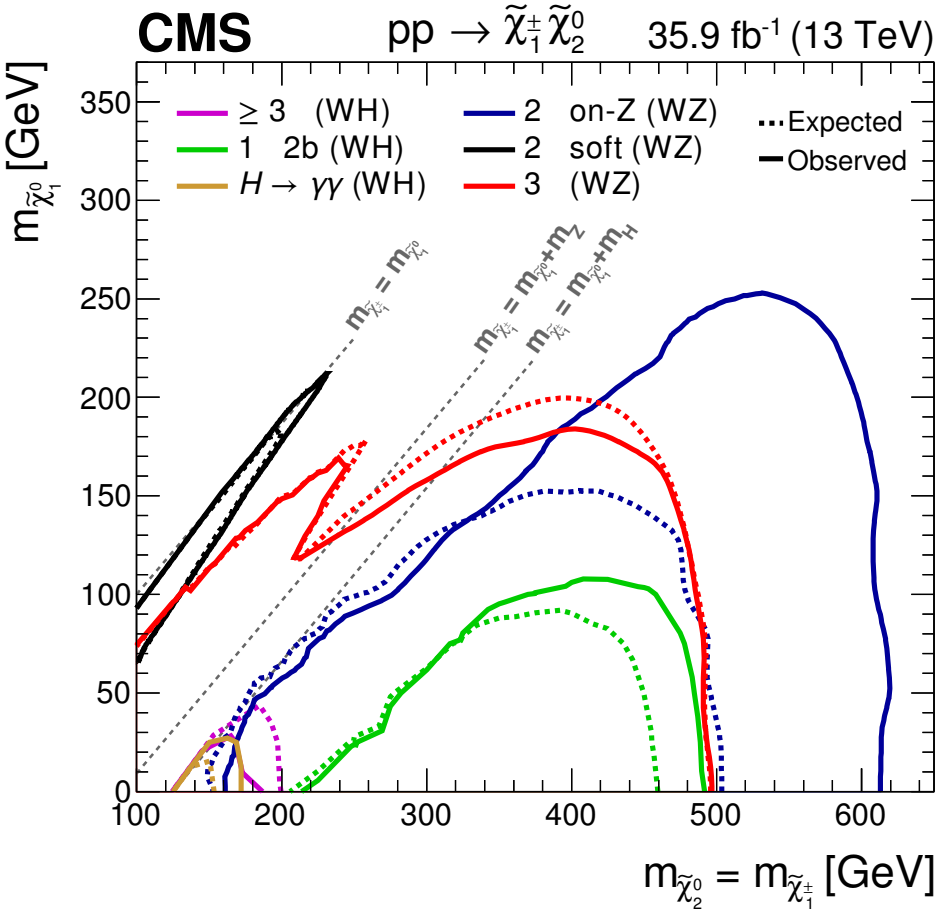

Figure 6

Mass reach of CMS searches for a selection of results targeting electroweak supersymmetry production, available as of December 2017 (124).

Standard Model leptons are light, and the search can benefit from a high leptonic branching ratio, whereas their reach is lower if their decays proceed through W and Z bosons. More luminosity also provides access to new regions of parameter space for specific signatures, such as so-called compressed regions where small mass differences between superpartners cause the signals to lie buried in large backgrounds at low $\not{E}_T$ (128, 129). Small mass differences can also suppress superpartner decays, resulting in long lifetimes that can be exploited to study regions with a mass difference as low as 0.2 GeV for higgsino models (130), in Fig.5. Other mechanisms of decay suppression can do this as well [e.g., split SUSY (131)].

Despite the unwieldy diversity SUSY signatures, a sufficiently specific model can provide a concrete framework on which to build an understanding of the combined effect of many experimental constraints. The study reported in Reference 132, continued by the LHC experimental collaborations (133, 134), uses the pMSSM to define a finite (although large)

parameter space for which the wealth of experimental constraints can be systematically evaluated, and underexamined signatures can be considered for future emphasis. One may also identify the LSP with astrophysical DM to focus more specifically on regions compatible with a given cosmology (e.g., 123).

Collaborations such as GAMBIT (135) and Mastercode (136) have combined a variety of tools to aid in such efforts. These codes encapsulate search results in statistical outputs that can be combined to construct global constraints for the models of interest. For example, one may compile the likelihood functions for the parameters of a SUSY model given the results from collider, DD, and ID experiments.

3.4. Searches for Long-Lived Particles

Prompt decays produce a visible recoil that originates at the collision point; thus, it can be reconstructed using the techniques for which the experiments were designed. The long-lived mediators described in Section 2.4 present different experimental challenges. For short lifetimes, LLPs can decay inside the tracking detectors, appearing as displaced decay vertices. Some SUSY decay chains lead to disappearing tracks, if the visible particles decay into the LSP and soft particles (e.g., 137,138). Even longer-lived particles can decay in the calorimeters or in the muon spectrometers, or they may exit the detector cavern completely before decaying. These signatures add yet another dimension of complexity to such searches, because observing these events may require dedicated triggers, reconstruction algorithms, and even detectors (139, 140).

Searches at colliders use a variety of experimental signatures to target different types of dark bosons, such as dark vector or scalar bosons. An LHCb search for dimuon resonances (141) is sensitive to visible decays of vector mediators in the mass range between 10 and 70 GeV. This search can use the entire sample of dimuon decays delivered to LHCb, recorded at the full collision rate directly at the trigger level (94), also placing constraints on dark bosons with longer lifetimes. Below 10 GeV, experiments at electron–positron colliders have searched for dilepton resonances or missing mass produced in association with ISR photons (e.g., 142, 143). LHCb also searches dimuon events for scalar bosons with masses between 250 MeV and 4.7 GeV (144), for a range of lifetimes. Dark bosons can also arise in Higgs decays via a hidden-sector mechanism. For example, the searches described in References 145 and 146 look for exotic Higgs decays into collimated lepton jets, constraining the decay rate to be below 10% for a range of dark photon lifetimes. Reference 65 provides a review of this and other possible benchmark models.

3.5. Consequences of Neutral-Mediated Models: Visible Decays

Dark interactions might also be probed without actually producing invisible particles. For example, if the mediator particle can be produced via interactions with quarks, it may also decay into quarks. In this case, it may be discovered in dijet, di–b jet, and ditop resonance searches (e.g., 38, 147).

Dijet resonance searches have been routinely used at hadron colliders to probe for heavy particles at newly reached collision energies. They exploit an expected absence of features in the dijet-invariant mass distribution to estimate the search background directly from a fit to the data, minimizing modeling and theory uncertainties. This permits the observation of low-rate localized excesses (width/mass of up to ∼15% and ∼30% for ATLAS and CMS respectively) from resonant dijet production (148, 149). For wider signals, searches

exploiting the scattering angle of dijet events can be used (148, 150).

At the LHC, typical dijet searches lose sensitivity at masses below approximately 1 TeV (151, 152), where high rates force the experiments to discard a large fraction of the data at the level of the trigger (see the sidebar titled Challenges for Triggering Low-Mass Resonances at Hadron Colliders). However, by recording much less information for these low-mass events (91,93), one can reduce this threshold to values as low as 450 GeV (95,149). Alternatively, one can look at the subset of dijet events in which a high-p_{T} ISR object happens to trigger (153, 154), in a similar fashion as in the jet+$\not{E}_T$ searches described in Section 3.2.1. LHC searches are sensitive to even lower mediator masses when reconstructing the mediator decay products into a single jet and employing substructure techniques (154, 155). Dedicated searches for resonances of third-generation quarks, with lower backgrounds and therefore lower thresholds, are also performed (156–158).

Resonance searches can also constrain mediator couplings to leptons (159, 160). For dielectron and dimuon searches, the main backgrounds arise from Drell–Yan processes, which are estimated with simulations corrected for next-to-next-to-leading-order effects and normalized to the Z boson yield in the data.

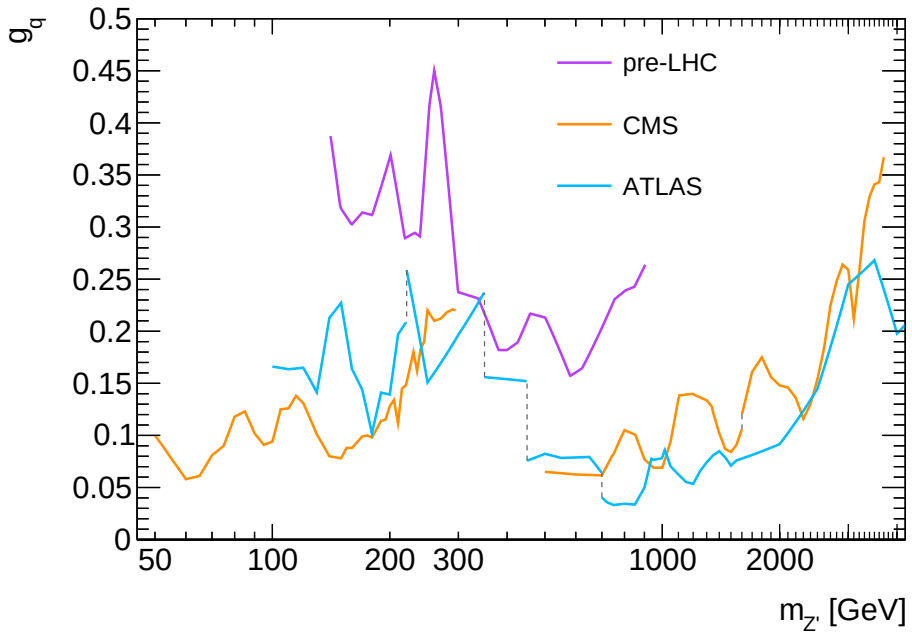

Figure 7

Summary of constraints from searches for light dijet resonances from ATLAS and CMS, where discrete points are taken from the coupling-mass limits on a simplified model mediated by an axial–vector Z' coupling exclusively to quarks from the searches mentioned in the text, and interpolated at the crossings. Couplings above the lines are excluded at 95% CL, up to the values where larger couplings yield a resonance width larger than 15% (roughly $g_{\mathrm{q}} > 0.5$). Abbreviation: DM, dark matter. Pre-LHC constraints are from Reference 152.

Figure 7 illustrates constraints from the dijet resonance searches mentioned above, on the quark coupling of the mediator in an axial–vector simplified model, as a function of the

mediator mass, for a model that assumes no tree-level couplings to leptons. This plot is made for a particular choice of DM mass, but would look similar for other DM masses. Searches for boosted mediator decays are sensitive to masses as low as 50 GeV and quark couplings g_q as low as 0.06 at 60 GeV. Jets from the mediator decay are spatially separated for mediator masses above 250–300 GeV, where the γ and gluon ISR+dijet channel constrains g_q to be greater than 0.15–0.2. Above 400 GeV, where searches with jets at the trigger level become available, they are the most sensitive, excluding g_q as low as 0.05. Above 1 TeV, standard dijet resonance and angular searches constrain quark couplings from 0.1 to unity, up to 5 TeV.

Mixing between this mediator and the Z boson induces loop-level couplings to leptons. ATLAS and CMS use several sets of coupling benchmarks to illustrate how the experimental constraints depend on these unknown values. For equal couplings of the mediator to leptons and jets, dilepton searches at a given mediator mass are far more sensitive than dijet searches. Other values are discussed further in the next section.

3.5.1. Comparison of the sensitivity of visible and invisible LHC searches. Fully visible signatures of a particular dark interaction can be powerful probes of it and, in some cases (e.g., when the invisible particles are too heavy to be directly produced), are the only way to observe dark interactions at a collider. By contrast, only $\not{E}_T$ searches can observe invisible-particle production directly. Each type of search complements the others; nevertheless, piecing together searches in different channels requires a model. Understanding precisely how these searches fit together can be challenging when the model is uncertain.

As an example, we again consider the case of vector or axial–vector mediators, to which both searches for anomalous $\not{E}_T$ and two-body resonance searches are sensitive. Although these models are simple, they involved four parameters: two couplings, the invisible-particle mass, and the mediator mass. Recent ATLAS and CMS results depict results in a two-dimensional plane of mediator mass and DM mass, following the recommendations of the LHC Dark Matter Working Group.[4] Figure 3.5.1 shows a sample of recent ATLAS plots. The remaining coupling parameters are fixed to one of several benchmark sets that are selected on the basis of the sensitivity of early Run 2 searches, precision constraints, and the complementarity of different types of searches. Figure 3.5.1 displays the constraints from dijet, dilepton, and $X+\not{E}_T$ searches on the interaction model as excluded regions of the model parameter space.

Figure 3.5.1*a* shows the LHC constraints in a scenario that privileges dijet decays, for couplings $g_q = 0.25$, $g_\ell = 0$, and $g_\chi = 1$. In this case, dijet searches exclude mediators between approximately 200 GeV and 2.6 TeV, while $X+\not{E}_T$ searches can constrain even lighter mediators. Figure 3.5.1*b* shows the exclusions for smaller quark couplings, $g_q = 0.1$, and a nonzero lepton coupling, $g_\ell = 0.01$, chosen as indicative of the possible size of loop-induced lepton couplings. With lower quark couplings, and thus lower dijet production and decay rates, the regions of masses excluded by the several dijet searches shrink. For mediators heavier than 150 GeV, the exclusions from the recent dilepton search fare better but do not extend very far into the (smaller) region excluded by the jet+$\not{E}_T$ search, where mediator decays to DM dominate.

Thus, the relative sensitivity of visible and invisible searches is both model and cou-

[4] Akin to simplified models of SUSY, where the axes are neutralino mass and superpartner particle mass.

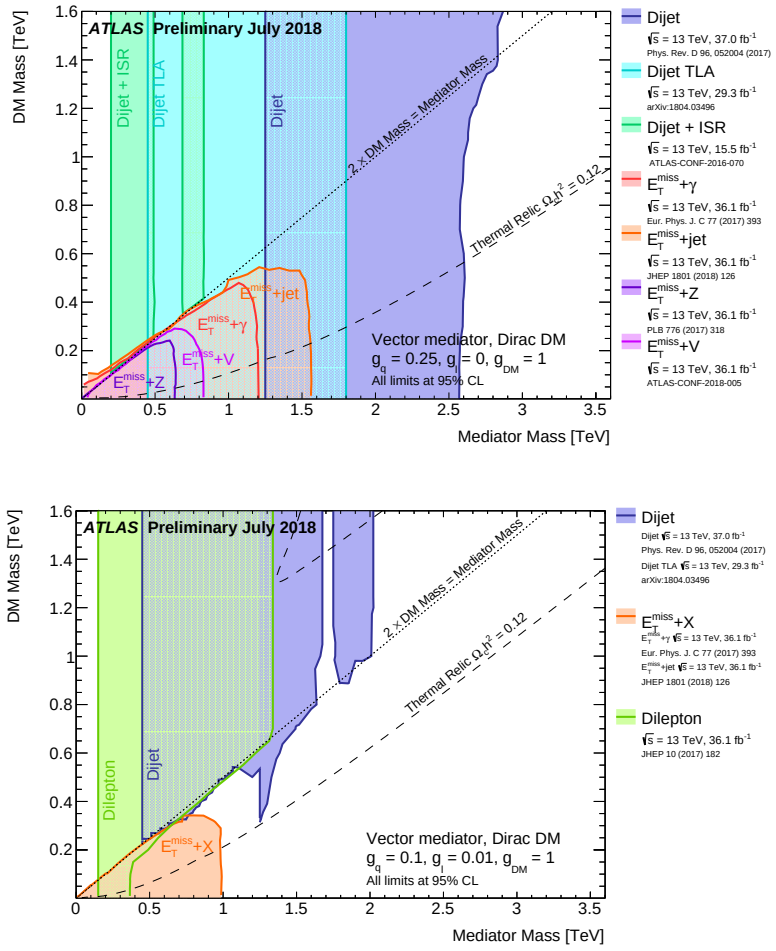

Regions in DM mass–Z' mediator mass excluded at 95% CL by a selection of ATLAS searches (from References (89, 95, 103, 106, 108, 148, 153, 159)) available as of July 2018, for two coupling scenarios. Dashed curves labeled "thermal relic" indicate combinations of DM and mediator mass that are consistent with a DM density of $\omega_c = 0.12h^2$ and a standard thermal history, as computed in MadDM for this model (161). The dotted curve indicates the kinematic threshold where the mediator can decay on-shell into DM. In panel (a), the couplings of the mediator particle to each generation of quarks (g_{q}) are set to 0.25, the couplings to leptons (g_ℓ) are set to zero and the coupling to DM is set to unity. In panel (b), g_{q} is set to 0.1, g_ℓ is set to 0.01 and the coupling to DM g_χ is set to unity and marked as g_{DM} in this plot. Abbreviations: DM, dark matter; ISR, initial-state radiation; TLA, trigger-object level analysis. Adapted from Reference 162.

pling dependent. One advantage of searches for invisible particles is their sensitivity to models with very light mediators (<50 GeV) and on-shell decays to DM, since the reach of dijet and dilepton searches to low-mass resonances is still ultimately limited by data-taking

constraints, but they are also stronger than direct mediator searches in the case of supersymmetric models (147). Further examples of complementarity can be found in other types of models, for example, in SUSY, where striking signatures of visible particle decays (e.g. same-sign dileptons or multiresonance final states) allow for discovery before more generic multijet + $\not{E}_T$ signatures (163).

Since we do not know what DM model is realized in nature, all of these search channels are potentially relevant, and have different strengths. They are all necessary for a thorough search program.

4. COMPARISON OF COLLIDER RESULTS WITH DIRECT AND INDIRECT DETECTION EXPERIMENTS

A wide variety of reactions may produce invisible particles at colliders, and if the mediators of the interaction are light enough to be produced on-shell, collider experiments are particularly well suited to discovering and characterizing the interactions responsible. Meanwhile, connecting a collider experiment's discovery or nondiscovery of invisible particles to DM requires both DD and ID experiments, wherein Galactic DM collides with a terrestrial target or extragalactic DM annihilates.

Making this connection requires that one assume a particle physics model. Within a given model and under well-specified assumptions, the information obtained in a collider experiment can be related to the information obtained in direct, indirect, and astrophysical probes, and vice versa. One can then compare and contrast the different types of information, for instance, to understand where a DM discovery in current DD searches could be further explored with mediator studies at the LHC, and where, among the multitude of possible signals, collider searches might focus their effort.

In the following subsections, we outline a strategy adopted by the ATLAS and CMS experiments when making comparisons with astrophysical observations (e.g., where a model is consistent with the present DM density in the Universe) and with DD and ID results. We discuss the assumptions made in the relic density calculation and in relating reactions for invisible particles to reactions of DM.

4.1. Comparing LHC Constraints from Visible- and Invisible-Particle Searches with Noncollider Results

The collider results from ATLAS and CMS typically appear as constraints on production cross sections of specific processes, which are then interpreted as statements about the fundamental parameters of a simplified model (e.g., masses, couplings). Within the model, information about the parameters can then be extrapolated to statements about the noncollider observable of interest—for example, the WIMP–nucleon scattering cross section for DD searches or the thermal relic density. The LHC Dark Matter Working Group (see Reference 39 and references therein) has provided instructions for how to perform these extrapolations. For the first, partial Run 2 LHC search results, generic searches have only selected models that had an early chance of discovery for these comparisons. But many other models can be used,[5] and published searches typically provide some form of model-

[5]For reinterpretation of LHC results and their comparisons to DD and ID searches for scalar and pseudoscalar mediators, as well as in the context of 2HDMs, see, for example, References 42,

agnostic results for this purpose.

For example, CMS and ATLAS have extrapolated the parameter exclusions obtained by a recent set of searches to the spin-independent WIMP–nucleon cross section of a DD experiment. The result for CMS is depicted in Figure 8, which shows a selection of DD results for comparison. The figure illustrates general features of many such comparisons.

For spin-dependent DD scattering, such as an axial–vector mediated model, the LHC signals are relatively insensitive to the Lorentz structure of the interaction, while the DD signals are suppressed. As a result, the corresponding plots show that LHC searches play a more powerful role relative to the DD searches over a wide range of invisible-particle masses. At intermediate DM masses, both LHC and DD experiments have great potential for a discovery and could verify one another's claims.

The LHC Dark Matter Working Group: provides for the translation of LHC limits to DD and ID searches (39), as well as calculations of relic density (see `https://gitlab.cern.ch/lhc-dmwg-material/relic-density`)

One can also compare collider and ID results using simplified model benchmarks. In traditional comparisons, only one DM annihilation state at a time was used for the comparison of collider and ID results, as in the case for $b\bar{b}$ (e.g., 116), but one can also compare ID and LHC results for models annihilating to multiple final-state fermions (166).

Recently, some DD and ID collaborations have adopted the benchmark simplified models used by ATLAS and CMS (e.g., 167, 168). IceCube and other experiments have used constraints from a MSSM scan (e.g., 169). The pMSSM is also a good framework to highlight the complementarity of LHC, DD, and ID experiments (e.g., 170).

We emphasize that the exclusion regions obtained in this way will depend strongly on the assumption of the model. The extrapolations are done with full knowledge that the simplified model is merely a crude guess, and one must be careful not to overgeneralize. Neither this procedure nor the simplified models themselves account for effects outside the model, such as interference and mixing with Standard Model boson and quarkonia resonances, or the evolution of the operators in the model from the LHC collision energies to other energy scales (171). Moreover, all experimental results, be they from DD, ID, or collider searches, are affected by experimental and theoretical uncertainties not shown in Figure 8. In principle, LHC $\not{E}_T$ searches cannot probe cases where WIMPs are so strongly interacting that they are stopped in the detector, see e.g. (172). LHC results haven't yet explicitly quoted an upper range to their bounds in Figure 8.

4.2. Relic Density Considerations

In the absence of a signal in noncollider experiments, the ability of a model to link its invisible particles with the observed DM abundance is key to distinguishing it from other types of models of BSM physics. Making this link, however, requires extrapolating from the present day to the early Universe along an increasingly tenuous chain of assumptions. For simplified models, this is especially problematic, because the model is designed to describe collider-scale processes; it may not even contain higher-scale interactions relevant in the early Universe.

Nevertheless, it is interesting to examine the parameter regions in models that can make the link, even if in limited situations (174, 175). For example, for the general simplified models discussed in Section 2.2.2, one can use programs such as MadDM and MicrOMEGas (161,176) to compute the DM abundance for a standard thermal relic, assuming that the interaction described by the simplified model is the one responsible for setting the

164, and 165.

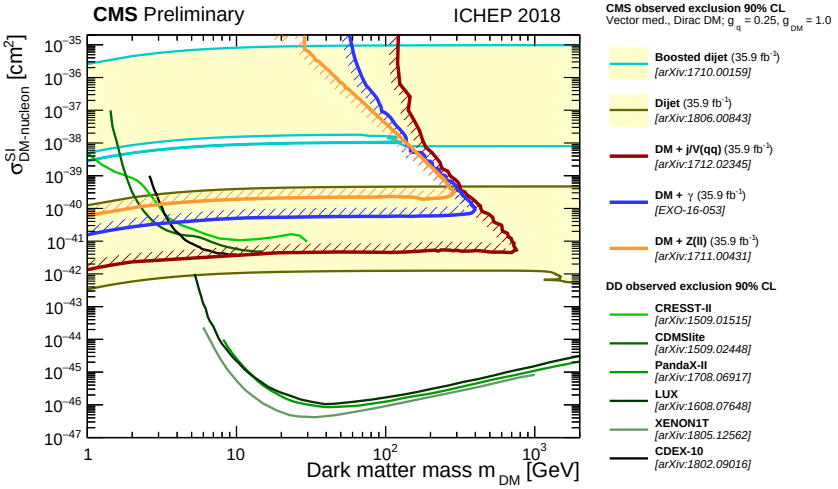

Figure 8

The 90%-CL constraints from the CMS experiment from References (**?**, 90, 102, 149, 154) in the m_χ-spin-independent DM–nucleon plane for a vector mediator, Dirac DM, and benchmark couplings $g_q = 0.25$ and $g_\chi = 1.0$ (marked as g_{DM} in this plot) chosen as an example of what early LHC searches would be sensitive to, compared with direct detection experiments from References (**?**, **?**, **?**, **?**, **?**). It is important to note that this comparison is only valid for this particular combination of model and parameter choices. Abbreviation: DM, dark matter. Adapted from Reference 173.

relic density. Often (e.g., Figure 3.5.1), ATLAS and CMS supplement their results with contours indicating where within a model this procedure obtains the correct DM density of $\omega_c = 0.12h^2$. These lines should be regarded as guidance rather than as strict requirements for the models considered. When the model cannot reproduce the correct abundance indicates either that the model requires additional components beyond those included in the simplified model or that the chain of assumptions is incorrect (11).

5. OUTLOOK

We are optimistic that, in the next decade, the variety of powerful searches for particle DM, from collider approaches to underground experiments to observatories, will lead to much progress toward its eventual discovery. Collider strategies that have been essential to discover and understand the fundamental particles of the Standard Model are being extended with new techniques designed to extract rare and difficult signals from the data. Our understanding of collider search targets is also rapidly improving. Along with SUSY benchmarks motivated by the hierarchy problem, targets directly motivated by DM observations are encouraging a new generation of experimentalists to branch out into directions that so far have been only sparsely explored. Finally, the HL-LHC data set will exceed that presented here by a factor of 100. These are exciting times (177).

FUTURE ISSUES

1. The obvious directions for LHC searches are toward lower-rate processes and processes that are more difficult to detect:
    - Extended scalar sectors and electroweak SUSY are among the possible benchmarks for lower rate processes. As the LHC experiments record progressively more data during Run 2 and Run 3, searches are becoming sensitive to the simplest scalar simplified models, opening the door to more realistic models. On a longer timescale, the HL-LHC data set will bring sensitivity up to 3 TeV in scalar mediator masses for unit couplings (178) and precision knowledge of the Standard Model Higgs sector, and the mass reach for electroweak production of SUSY partners should increase by a few hundred GeV (179).
    - With data arriving at a slightly less frantic pace, experimentally challenging LLP signatures are a growing field, and benchmarks similar to Reference 15 are needed to help guide the design of these searches. Among many ongoing efforts are the bottom-up approach adopted in Reference 180, which connects such models with the LLP limit of those described in Section 2.2.2. Many LLP searches have not yet been done, and not all existing searches have been optimized. Therefore, LLP searches have the potential for substantial improvements, much beyond those expected by the accumulation of luminosity.
2. Precision searches, detector upgrades, and efficient triggering of rare signals buried in large backgrounds are key to fully exploiting the HL-LHC data set:
    - In the familiar jet+$\not{E}_T$ search, precision estimates of the V+jet backgrounds, and of the inputs to these predictions, will be crucial. Efforts in that direction are ongoing (181).
    - Upgrades for Run 3 and HL-LHC provide new capabilities that may make new data more valuable for these searches than what recorded so far for rare processes involving light new particles. This is a subject that has been largely unexplored for ATLAS and CMS (182) and that can be developed further when tracking information is available at the trigger level to remove pileup. LHCb will make use of a novel triggerless detector readout to perform dark photon searches with unprecedented sensitivities (183).
3. Future hadron and electron–positron colliders have immense potential [see, e.g., studies on a future hadron collider (184)]. Nevertheless, present studies largely continue the approaches already in use at the LHC. A new hadron collider would be built to discover New Physics; therefore, qualitatively different experimental design, benchmark models, and analysis strategies should be considered.
4. More useful working comparisons between results from colliders, underground searches, and observatories should take into account the uncertainties on each type of result, and on the extrapolations between them. The main uncertainties for LHC searches are outlined in Section 3 and in the experimental references; for a summary of DD and ID uncertainties, see References 185 and 186 and references therein.
5. Comparisons among collider and noncollider particle physics experiments are becoming standard; relating particle physics to astrophysical observables is crucial to

exploit the few clues that DM can provide about BSM particle physics. We strongly encourage further research on this subject (e.g., 187).

DISCLOSURE STATEMENT

The authors are not aware of any affiliations, memberships, funding, or financial holdings that might be perceived as affecting the objectivity of this review.

ACKNOWLEDGMENTS

We thank William Kalderon, Teng Jian Khoo, Suchita Kulkarni, Priscilla Pani, Frederik Ruehr, Tim Tait, Emma Tolley, Liantao Wang, and Bryan Zaldivar for their help and advice in preparing this manuscript. We also thank Ulrich Haisch, Valerio Ippolito, Christian Ohm, Jessie Shelton, and Mike Williams for useful discussion. Research by A.B. is supported by the US Department of Energy (grant DE-SC0011726). Research by C.D. is part of a project that has received funding from the European Research Council under the European Union's Horizon 2020 research and innovation program (grant agreement 679305) and from the Swedish Research Council.

LITERATURE CITED

1. Bertone G, Hooper D, Silk J. *Phys. Rep.* 405:279 (2005)
2. Cohen T, et al. *Phys. Rev. Lett.* 119:021102 (2017)
3. Ellis JR, Falk T, Olive KA, Srednicki M. *Astropart. Phys.* 13:181 (2000); Erratum. *Astropart. Phys.* 15:413 (2001)
4. Ade PAR, et al. *Astron. Astrophys.* 594:A13 (2016)
5. Undagoitia TM, Rauch L. *J. Phys. G* 43:013001 (2016)
6. Gaskins JM. *Contemp. Phys.* 57:496 (2016)
7. ATLAS Collab. *J. Instrum.* 3:S08003 (2008)
8. CMS Collab. *J. Instrum.* 3:S08004 (2008)
9. LHCb Collab. *J. Instrum.* 3:S08005 (2008)
10. Steigman G, Dasgupta B, Beacom JF. *Phys. Rev. D* 86:023506 (2012)
11. Bernal N, et al. *Int. J. Mod. Phys. A* 32:1730023 (2017)
12. Brooijmans G, et al. arXiv:1803.10379 [hep-ph] (2018)
13. Evans JA, Gori S, Shelton J. *J. High Energy Phys.* 1802:100 (2018)
14. D'Ambrosio G, Giudice GF, Isidori G, Strumia A. *Nucl. Phys. B* 645:155 (2002)
15. Abercrombie D, et al. arXiv:1507.00966 [hep-ex] (2015)
16. Patt B, Wilczek F. arXiv:hep-ph/0605188 (2006)
17. Djouadi A, Lebedev O, Mambrini Y, Quevillon J. *Phys. Lett. B* 709:65 (2012)
18. Escudero M, Berlin A, Hooper D, Lin MX. *J. Cosmol. Astropart. Phys.* 1612:029 (2016)
19. Goodman J, et al. *Phys. Rev. D* 82:116010 (2010)
20. Bai Y, Fox PJ, Harnik R. *J. High Energy Phys.* 1012:048 (2010)
21. Fox PJ, Harnik R, Kopp J, Tsai Y. *Phys. Rev. D* 85:056011 (2012)
22. Beltran M, et al. *J. High Energy Phys.* 1009:037 (2010)
23. Shoemaker IM, Vecchi L. *Phys. Rev. D* 86:015023 (2012)
24. Racco D, Wulzer A, Zwirner F. *J. High Energy Phys.* 1505:009 (2015)

25. Busoni G, De Simone A, Morgante E, Riotto A. *Phys. Lett. B* 728:412 (2014)
26. Alwall J, Schuster P, Toro N. *Phys. Rev. D* 79:075020 (2009)
27. LHC New Phys. Work. Group. *J. Phys. G* 39:105005 (2012)
28. DiFranzo A, Nagao KI, Rajaraman A, Tait TMP. *J. High Energy Phys.* 1311:014 (2013); Erratum. *J. High Energy Phys.* 1401:162 (2014)
29. Abdallah J, et al. *Phys. Dark Univ.* 9/10:8 (2015)
30. Kahlhoefer F, Schmidt-Hoberg K, Schwetz T, Vogl S. *J. High Energy Phys.* 02:016 (2016)
31. Backovic M, et al. *Eur. Phys. J. C* 75:482 (2015)
32. Papucci M, Vichi A, Zurek KM. *J. High Energy Phys.* 1411:024 (2014)
33. An H, Wang LT, Zhang H. *Phys. Rev. D* 89:115014 (2014)
34. Bell NF, et al. *Phys. Rev. D* 86:096011 (2012)
35. Han C, Lee HM, Park M, Sanz V. *Phys. Lett. B* 755:371 (2016)
36. Albert A, et al. arXiv:1703.05703 [hep-ex] (2017)
37. Berlin A, Lin T, Wang LT. *J. High Energy Phys.* 1406:078 (2014)
38. Chala M, et al. *J. High Energy Phys.* 1507:089 (2015)
39. Boveia A, et al. arXiv:1603.04156 [hep-ex] (2016)
40. Buckley MR, Feld D, Goncalves D. *Phys. Rev. D* 91:015017 (2015)
41. Haisch U, Re E. *J. High Energy Phys.* 1506:078 (2015)
42. Bell NF, Busoni G, Sanderson IW. *J. Cosmol. Astropart. Phys.* 1703:015 (2017)
43. Albert A, et al. *Phys. Dark Univ.* 16:49 (2017)
44. Englert C, McCullough M, Spannowsky M. *Phys. Dark Univ.* 14:48 (2016)
45. Bai Y, Berger J. *J. High Energy Phys.* 11:171 (2013)
46. Ko P, Natale A, Park M, Yokoya H. *J. High Energy Phys.* 01:086 (2017)
47. Blanke M, Kast S. *J. High Energy Phys.* 05:162 (2017)
48. Boucheneb I, Cacciapaglia G, Deandrea A, Fuks B. *J. High Energy Phys.* 01:017 (2015)
49. Buschmann M, et al. *J. High Energy Phys.* 09:033 (2016)
50. Khoze VV, Plascencia AD, Sakurai K. *J. High Energy Phys.* 06:041 (2017)
51. Bauer M, Haisch U, Kahlhoefer F. *J. High Energy Phys.* 05:138 (2017)
52. Goncalves D, Machado PAN, No JM. *Phys. Rev. D* 95:055027 (2017)
53. Pich A, Tuzon P. *Phys. Rev. D* 80:091702 (2009)
54. Duerr M, et al. *J. High Energy Phys.* 09:042 (2016)
55. Feng JL. *Annu. Rev. Astron. Astrophys.* 48:495 (2010)
56. Ellis J, et al. *Nucl. Phys. B* 238:453 (1984)
57. Farrar GR, Fayet P. *Phys. Lett. B* 76:575 (1978)
58. Dimopoulos S, Dine M, Raby S, Thomas SD. *Phys. Rev. Lett.* 76:3494 (1996)
59. Masiero A, Profumo S, Ullio P. *Nucl. Phys. B* 712:86 (2005)
60. Pospelov M, Ritz A, Voloshin MB. *Phys. Lett. B* 662:53 (2008)
61. Das S, Sigurdson K. *Phys. Rev. D* 85:063510 (2012)
62. Co RT, D'Eramo F, Hall LJ, Pappadopulo D. *J. Cosmol. Astropart. Phys.* 1512:024 (2015)
63. Kahlhoefer F. *Phys. Lett. B* 779:388 (2018)
64. Holdom B. *Phys. Lett. B* 166:196 (1986)
65. Curtin D, Essig R, Gori S, Shelton J. *J. High Energy Phys.* 02:157 (2015)
66. Battaglieri M, et al. arXiv:1707.04591 [hep-ph] (2017)
67. El Hedri S, Kaminska A, de Vries M, Zurita J. *J. High Energy Phys.* 04:118 (2017)
68. Strassler MJ, Zurek KM. *Phys. Lett. B* 651:374 (2007)
69. Zurek KM. *Phys. Rep.* 537:91 (2014)
70. Craig N, Knapen S, Longhi P. *Phys. Rev. Lett.* 114:061803 (2015)
71. Hochberg Y, Kuflik E, Volansky T, Wacker JG. *Phys. Rev. Lett.* 113:171301 (2014)
72. Schael S, et al. *Phys. Rep.* 427:257 (2006)
73. Carena M, de Gouvea A, Freitas A, Schmitt M. *Phys. Rev. D* 68:113007 (2003)
74. ATLAS Collab. *Eur. Phys. J. C* 77:765 (2017)

75. ATLAS Collab., CMS Collab. *J. High Energy Phys.* 08:045 (2016)
76. ATLAS Collab. *J. High Energy Phys.* 11:206 (2015)
77. Dobrescu BA, Lykken JD. *J. High Energy Phys.* 1302:073 (2013)
78. CMS Collab. *J. High Energy Phys.* 02:135 (2017)
79. Fox PJ, Harnik R, Kopp J, Tsai Y. *Phys. Rev. D* 84:014028 (2011)
80. Birkedal A, Matchev K, Perelstein M. *Phys.Rev. D* 70:077701 (2004)
81. ATLAS Collab. *Eur. Phys. J. C* 77:241 (2017)
82. CMS Collab. *Performance of missing energy reconstruction in 13 TeV* pp *collision data using the CMS detector*. Report CMS-PAS-JME-16-004, CERN, Geneva (2016)
83. ATLAS Collab. *Pile-up suppression in missing transverse momentum reconstruction in the ATLAS experiment in proton–proton collisions at* $\sqrt{s}$ *= 8 TeV*. Report ATLAS-CONF-2014-019, CERN, Geneva (2014)
84. ATLAS Collab. *Selection of jets produced in 13 TeV proton–proton collisions with the ATLAS detector*. Report ATLAS-CONF-2015-029, CERN, Geneva (2015)
85. ATLAS Collab. *Phys. Rev. D* 94:032005 (2016)
86. Haisch U, Kahlhoefer F, Re E. *J. High Energy Phys.* 1312:007 (2013)
87. Smith WH. *Annu. Rev. Nucl. Part. Sci.* 66:123 (2016)
88. Aaij R, et al. *J. Instrum.* 8:P04022 (2013)
89. ATLAS Collab. *J. High Energy Phys.* 1801:126 (2018)
90. CMS Collab. *Phys. Rev. D* 97:092005 (2018)
91. ATLAS Collab. *Eur. Phys. J. C* 77:317 (2017)
92. CMS Collab. *J. Instrum.* 12:P01020 (2017)
93. CMS Collab. *Phys. Rev. Lett.* 117:031802 (2016)
94. LHCb Collab. *Comput. Phys. Commun.* 208:35 (2016)
95. ATLAS Collab. arXiv:1804.03496 [hep-ex] (2018)
96. CMS Collab. *Pileup removal algorithms*. Report CMS-PAS-JME-14-001, CERN, Geneva (2014)
97. ATLAS Collab. *Fast TracKer (FTK) technical design report*. Report CERN-LHCC-2013-007/ATLAS-TDR-021, CERN, Geneva (2013)
98. CMS Collab. *J. Instrum.* 6:C12065 (2011)
99. Lindert JM, et al. *Eur. Phys. J. C* 77:829 (2017)
100. Maguire E, Heinrich L, Watt G. *J. Phys. Conf. Ser.* 898:102006 (2017)
101. CMS Collab. *Simplified likelihood for the re-interpretation of public CMS results*. Report CMS-NOTE-2017-001, CERN, Geneva (2017)
102. CMS Collab. *Eur. Phys. J. C* 78:291 (2018)
103. ATLAS Collab. *Phys. Lett. B* 776:318 (2018)
104. Gershtein Y, Petriello F, Quackenbush S, Zurek KM. *Phys. Rev. D* 78:095002 (2008)
105. Petriello FJ, Quackenbush S, Zurek KM. *Phys. Rev. D* 77:115020 (2008)
106. ATLAS Collab. *Eur. Phys. J. C* 77:393 (2017)
107. CMS Collab. *Search for dark matter and large extra dimensions in the* $\gamma + \not{E}_T$ *final state in pp Collisions at* $\sqrt{s}$*=13 TeV*. Report CMS-PAS-EXO-16-014, CERN, Geneva (2016)
108. ATLAS Collab. *Search for dark matter in events with a hadronically decaying vector boson and missing transverse momentum in pp collisions at* $\sqrt{s} = 13$ *TeV with the ATLAS detector*. Report ATLAS-CONF-2018-005, CERN, Geneva (2016)
109. Larkoski AJ, Moult I, Nachman B. arXiv:1709.04464 [hep-ph] (2017)
110. CMS Collab. *Search for dark matter produced in association with a Higgs boson decaying to two photons*. Report CMS-PAS-EXO-16-054, CERN, Geneva (2017)
111. ATLAS Collab. *Phys. Rev. D* 96:112004 (2017)
112. ATLAS Collab. *Phys. Rev. Lett.* 119:181804 (2017)
113. ATLAS Collab. *Eur. Phys. J. C* 78:18 (2018)
114. ATLAS Collab. arXiv:1711.11520 [hep-ex] (2017)

115. CMS Collab. *Phys. Rev. D* 97:032009 (2018)
116. Agrawal P, Batell B, Hooper D, Lin T. *Phys. Rev. D* 90:063512 (2014)
117. CMS Collab. arXiv:1801.08427 [hep-ex] (2018)
118. ATLAS Collab. *Eur. Phys. J. C* 75:79 (2015)
119. Lester CG, Summers DJ. *Phys. Lett. B* 463:99 (1999)
120. ATLAS Collab. *Phys. Rev. D* 96:112010 (2017)
121. CMS Collab. *J. High Energy Phys.* 12:142 (2017)
122. CMS Collab. *J. High Energy Phys.* 10:005 (2017)
123. ATLAS Collab. *J. High Energy Phys.* 09:175 (2016)
124. CMS Collab. *Supersymmetry public results*. CERN, Geneva. `https://twiki.cern.ch/twiki/bin/view/CMSPublic/PhysicsResultsSUS` (2018)
125. ATLAS Collab. *Supersymmetry public results*. CERN, Geneva. `https://twiki.cern.ch/twiki/bin/view/AtlasPublic/SupersymmetryPublicResults` (2018)
126. CMS Collab. arXiv:1801.03957 [hep-ex] (2018)
127. ATLAS Collab. *Search for electroweak production of supersymmetric particles in the two and three lepton final state at $\sqrt{s}$=13 TeV with the ATLAS detector*. Report ATLAS-CONF-2017-039, CERN, Geneva (2017)
128. ATLAS Collab. arXiv:1712.08119 [hep-ex] (2017)
129. CMS Collab. *J. High Energy Phys.* 11:029 (2017)
130. ATLAS Collab. *Search for direct pair production of higgsinos by the reinterpretation of the disappearing track analysis with 36.1 fb^{-1} of $\sqrt{s}$ = 13 TeV data collected with the ATLAS experiment* Report ATL-PHYS-PUB-2017-019 (2017)
131. CMS Collab. arXiv:1802.02110 [hep-ex] (2018)
132. Conley JA, et al. *Eur. Phys. J. C* 71:1697 (2011)
133. ATLAS Collab. *J. High Energy Phys.* 10:134 (2015)
134. CMS Collab. *J. High Energy Phys.* 10:129 (2016)
135. GAMBIT Collab. *Eur. Phys. J. C* 77:784 (2017)
136. Mastercode Collab. arXiv:1710.11091 [hep-ph] (2017)
137. ATLAS Collab. arXiv:1712.02118 [hep-ex] (2017)
138. CMS Collab. *J. High Energy Phys.* 01:096 (2015)
139. Ball A, et al. arXiv:1607.04669 [physics.ins-det] (2016)
140. Chou JP, Curtin D, Lubatti HJ. *Phys. Lett. B* 767:29 (2017)
141. LHCb Collab. arXiv:1710.02867 [hep-ex] (2017)
142. BaBar Collab. *Phys. Rev. Lett.* 113:201801 (2014)
143. BaBar Collab. *Phys. Rev. Lett.* 119:131804 (2017)
144. LHCb Collab. *Phys. Rev. D* 95:071101 (2017)
145. ATLAS Collab. *Search for long-lived neutral particles decaying into displaced lepton jets in proton–proton collisions at $\sqrt{s}$ = 13 TeV with the ATLAS detector*. Report ATLAS-CONF-2016-042, CERN, Geneva (2016)
146. CMS Collab. *A search for beyond Standard Model light bosons decaying into muon pairs*. Report CMS-PAS-HIG-16-035, CERN, Geneva (2016)
147. Liew SP, Papucci M, Vichi A, Zurek KM. *J. High Energy Phys.* 06:082 (2017)
148. ATLAS Collab. *Phys. Rev. D* 96:052004 (2017)
149. CMS Collab. arXiv:1806.00843 [hep-ex] (2018)
150. CMS Collab. *Search for new physics with dijet angular distributions in proton–proton collisions at $\sqrt{s}$=13 TeV and constraints on dark matter and other models*. Report CMS-PAS-EXO-16-046, CERN, Geneva (2017)
151. An H, Huo R, Wang LT. *Phys. Dark Univ.* 2:50 (2013)
152. Dobrescu BA, Yu F. *Phys. Rev. D* 88:035021 (2013); Erratum. *Phys. Rev. D* 90:079901 (2014)
153. ATLAS Collab. *Search for new light resonances decaying to jet pairs and produced in association with a photon or a jet in proton–proton collisions at $\sqrt{s}$ = 13 TeV with the ATLAS*

detector. Report ATLAS-CONF-2016-070, CERN, Geneva (2016)
154. CMS Collab. arXiv:1710.00159 [hep-ex] (2017)
155. ATLAS Collab. arXiv:1801.08769 [hep-ex] (2018)
156. CMS Collab. *Search for a narrow heavy decaying to bottom quark pairs in the 13 TeV data sample*. Report CMS-PAS-HIG-16-025, CERN, Geneva (2016)
157. ATLAS Collab. *Phys. Rev. Lett.* 119:191803 (2017)
158. ATLAS Collab. arXiv:1805.09299 [hep-ex] (2018)
159. ATLAS Collab. *J. High Energy Phys.* 10:182 (2017)
160. CMS Collab. *Phys. Lett. B* 768:57 (2017)
161. Backovic M, et al. *Phys. Dark Univ.* 9/10:37 (2015)
162. ATLAS Collab. *Summary plots from the ATLAS exotic physics group*. CERN, Geneva. `https://atlas.web.cern.ch/Atlas/GROUPS/PHYSICS/CombinedSummaryPlots/EXOTICS/index.html#ATLAS_DarkMatter_Summary` (2017)
163. Acharya BS, et al. arXiv:0901.3367 [hep-ph] (2009)
164. GAMBIT Collab. *Eur. Phys. J. C* 77:568 (2017)
165. Banerjee S, et al. *J. High Energy Phys.* 07:080 (2017)
166. Carpenter LM, Colburn R, Goodman J, Linden T. *Phys. Rev. D* 94:055027 (2016)
167. PICO Collab. *Phys. Rev. Lett.* 118:251301 (2017)
168. Balazs C, et al. *Phys. Rev. D* 96:083002 (2017)
169. Aartsen MG, et al. *Eur. Phys. J. C* 77:146 (2017)
170. Cahill-Rowley M, Hewett JL, Ismail A, Rizzo TG. *Phys. Rev. D* 91:055002 (2015)
171. D'Eramo F, Procura M. *J. High Energy Phys.* 04:054 (2015)
172. N. Daci, I. De Bruyn, S. Lowette, M. H. G. Tytgat and B. Zaldivar, JHEP **1511**, 108 (2015)
173. CMS Collab. *Dark matter summary plots from CMS for LHCP and EPS 2017*. CERN, Geneva. `https://twiki.cern.ch/twiki/pub/CMSPublic/PhysicsResultsEXO/DM-summary-plots-Jul17.pdf` (2017)
174. Busoni G, et al. *J. Cosmol. Astropart. Phys.* 1503:022 (2015)
175. Catena R, Conrad J, Krauss MB. arXiv:1712.07969 [hep-ph] (2017)
176. Barducci D, et al. *Comput. Phys. Commun.* 222:327 (2018)
177. Steigman G. *Annu. Rev. Nucl. Part. Sci.* 29:313 (1979)
178. CMS Collab. *Estimated sensitivity for new particle searches at the HL-LHC*. Tech. rep. CMS-PAS-FTR-16-005, CERN, Geneva (2017)
179. Campana P, Klute M, Wells P. *Annu. Rev. Nucl. Part. Sci.* 66:273 (2016)
180. Buchmueller O, et al. *J. High Energy Phys.* 09:076 (2017)
181. Blumenschein U, et al. arXiv:1802.02100 [hep-ex] (2018)
182. Alves A, et al. *J. High Energy Phys.* 04:164 (2017)
183. Ilten P, et al. *Phys. Rev. Lett.* 116:251803 (2016)
184. Golling T, et al. In *CERN Yellow Report*, ed. ML Mangano, p. 441. Geneva: CERN (2017)
185. Feldstein B, Kahlhoefer F. *J. Cosmol. Astropart. Phys.* 1412:052 (2014)
186. Auchettl K, Balazs C. Uncertainties in dark matter indirect detection. In *Open Questions in Cosmology*, ed. GJ Olmo, pp. 87–110. London: IntechOpen (2012)
187. Buckley MR, Peter AHG. arXiv:1712.06615 [astro-ph.CO] (2017)

RELATED RESOURCES

1. Bertone G, et al. *Particle Dark Matter: Observations, Models and Searches*. Cambridge, UK: Cambridge Univ. Press (2010)
2. Bertone G, Hooper D. arXiv:1605.04909 [astro-ph.CO] (2016)
3. Plehn T. *Yet another introduction to dark matter*. Lect. notes, Inst. Theor. Phys., Univ. Heidelberg, Ger. `http://www.thphys.uni-heidelberg.de/~plehn/`

pics/dark_matter.pdf (2017)
4. Arcadi G, et al. arXiv:1703.07364 [hep-ph] (2017)
5. Kahlhoefer F. *Int. J. Mod. Phys. A* 32:1730006 (2017)
6. LHC Physics Center CERN. *WG on dark matter searches at the LHC*. DMWG Work. Group home page, CERN, Geneva. http://lpcc.web.cern.ch/content/lhc-dm-wg-wg-dark-matter-searches-lhc (2015)